Petroleum Exploration Enhancement Program (PEEP)
Project 2016-2017 Report

Reservoir quality and porosity evolution of Cambrian and Ordovician rift-drift and foreland basin sandstones, western Newfoundland

* Stefanie Lode and Luke Beranek, Dept. of Earth Sciences, Memorial University

(slode@mun.ca, 697-9082; lberanek@mun.ca, 864-4588)

Introduction

The Anticosti Basin is a Paleozoic depocentre in western Newfoundland that contains conventional and unconventional hydrocarbon plays (Hinchey et al., 2015; Hogg et al., 2015). Petroleum exploration activity in the Anticosti Basin has historically focused on the Port au Port (Anticosti south), Bay of Islands (Anticosti central), and Northern Peninsula areas (Anticosti north; Hicks and Owens, 2014; Waldron et al., 2012). The Anticosti Basin in the Port au Port peninsula area hosts five conventional plays that are predominantly within Ordovician St. George Group carbonate shelf rocks (Aguathuna, Catoche, Boat Harbour, and Watts Bight) and Cambrian Hawke Bay Formation shallow-marine strata (Cooper et al., 2001; Hogg et al., 2015). Middle Ordovician to Devonian foreland basin flysch (Goose Tickle Group and Misty Point, Clam Bank, and Red Island Road formations) represent further clastic reservoirs in the Port au Port peninsula area (Dietrich et al., 2011). Petroleum plays in the Humber Arm allochthon near eastern Port au Port Bay and Bay of Islands are hosted within Eagle Island Formation turbidites (correlative with Goose Tickle Group) and rift-drift strata of the Cambrian Blow Me Down Brook Formation (Hicks and Owens 2014; Dietrich et al., 2011).

The foci of this research project are Cambrian sandstone reservoirs of the Hawke Bay (autochthonous shelf) and correlative Blow Me Down Brook (Humber Arm allochthon slope and rise) formations, and Ordovician sandstone reservoirs of the Goose Tickle Group (autochthonous shelf) and Eagle Island formation (Humber Arm allochthon) in the Port au Port peninsula and Bay of Islands areas (Fig. 1). The purpose of this project is to apply an integrated field and laboratory approach to quantify the reservoir quality and porosity evolution of rift-drift to early-shelf and foreland basin strata in western Newfoundland. The source-to-sink characteristics of these onshore sandstones and their depositional environments are also addressed within the framework of this project. The research consists of stratigraphic field mapping, thin section petrography, and advanced SEM-MLA (scanning electron microscopy-mineral liberation analysis) micro-analytical imaging methodologies. SEM-MLA produces high-resolution digital maps of scanned thin-sections (or rock cuttings) that quantify the modal mineralogy, effective porosity, sorting, and grain-composition, -size, and -shape, including dissolution/ precipitation reactions, of a rock sample. The gained results provide information regarding the provenance of the studied west-derived Cambrian rift-drift-shelf shallow- to deeper-marine and east-derived Ordovician foreland basin sandstones in the Port au Port and Bay of Islands areas. Thus, the results of this study are of significance not only for occurrences of rift-drift and foreland basin sandstones within the Bay of Islands and Port au Port peninsula areas, but also have exploration implications for other conventional sandstone reservoirs globally.

Regional Geology

Western Newfoundland is located in the Cambrian (~515 Ma) to Permian (~275 Ma) Caledonian-Appalachian mountain belt and typically divided into four tectonostratigraphic zones (from west to east): Humber, Dunnage, Gander, and Avalon (Fig. 1; Williams, 1979; van Staal and Barr, 2011). These zones result from and were affected by the successive accretion of three micro-continental blocks during the early to mid-Paleozoic (i.e., Dashwoods, Taconic orogenesis; Ganderia, Salinic orogenesis; and Avalonia, Acadian orogenesis) and related interoceanic arcs and backarcs (Cooper et al., 2001; Zagorevski et al*.,* 2010). These ribbon-shaped micro-continental blocks separated from Gondwana and Laurentia during the early Paleozoic, forming pericratonic terranes that subsequently accreted to the composite Appalachian margin (e.g., van Staal and Barr 2011).

The Humber Zone is the westernmost tectonostratigraphic domain and mostly consists of Cambrian-Ordovician rift to passive margin and Ordovician-Devonian foreland basin strata that were deposited on Grenvillian basement (Fig. 1; Quinn, 1985; Cooper et al., 2001; Lavoie et al., 2003; van Staal and Barr, 2011). The Humber Zone records multiphase deformation during the three late Cambrian to Late Ordovician (495-450 Ma) Taconic, early Silurian (440-423 Ma) Salinic, and the latest Silurian to Middle Devonian (421-380 Ma) Acadian orogenic events (Cooper et al. 2001; van Staal and Barr, 2011). The Grenvillian crystalline basement comprises Mesoproterozoic igneous and metamorphic rocks and is predominantly exposed as structural inliers (Fig. 1; van Staal and Barr 2011; Waldron et al., 2012). Overall, the Humber Zone is characterized by a complex stacking of tectonic slices, including the basement, platform, slope, rise, and shallow to deep foreland basin units (Lavoie et al., 2003, Waldron et al., 2003). Structures in the Humber Zone originally developed during the Taconic orogeny and were reactivated during Salinic and Acadian orogenies (Stockmal and Waldron, 1990; Waldron et al., 2003, 2012). These structures are characterised by the emplacement of out of sequence thrust sheets and normal faulting with reverse-sense fault reactivation, including thick-skinned thrusting (Stockmal and Waldron, 1990; Waldron et al., 2003; Dietrich et al., 2011, Waldron et al., 2012).

Between the latest Neoproterozoic (~600 Ma) and Early Ordovician (~470 Ma), the deposition of rift and shelf succession strata occurred along the Laurentian shelf, whereby a thick carbonate-dominated succession overlies lower Cambrian clastic sedimentary rocks (Lavoie et al., 2003; Waldron et al., 2012). Contemporary with these shallow-water strata, deeper-water facies were deposited on the continental slope and rise and are preserved in the Humber Arm Supergroup, which, together with the ophiolite complexes, comprise the Humber Arm allochthon (Fig. 2; e.g., Waldron et al., 2012). The Bay of Islands and Little Port ophiolite complexes derived from island arcs southeast of the Laurentian margin and were thrust above the shelf succession and now represent the structurally highest tectonic slices of the Humber Arm allochthon (Lindholm and Casey, 1990; Burden et al., 2005; Waldron et al., 2003, 2012). The emplacement of thrust sheets during the early phases of the Taconic orogeny created a flexural forebulge and caused the formation of shallow to deep foreland basins that onlapped the shelf during the Ordovician and again during the latest Silurian to Early Devonian (Cooper et al., 2001; Lavoie et al., 2003; Waldron et al., 2012). Non-marine clastic sedimentary rocks, marine limestone, evaporites, and coal of the late Paleozoic Maritimes Basin overly the deformed Appalachian rocks and represent the fill of a successor basin (Cooper et al., 2001; Waldron et al., 2012).

Autochthonous successions

The autochthonous St. Lawrence platform extends from southern Quebec to western Newfoundland and is in tectonic contact (Appalachian structural front) with the Humber Zone

(Lavoie et al., 2003; Dietrich et al., 2011). Lower to middle Cambrian shelf and rift-related rocks of the Labrador Group comprise the base of the autochthonous shelf succession in the Port au Port area (James et al., 1989; Waldron et al., 2003; Conliffe et al., 2017). Late Proterozoic to early Cambrian rifting and opening of the Iapetus Ocean created the accommodation space for transgressive fluvial to marine arkosic sandstone of the Bradore Formation, lower Labrador Group (Cooper et al., 2001; Waldron et al., 2003; Dietrich et al., 2011). The base of the Bradore Formation is marked by an unconformity that represents a regional seismic reflector (Cooper et al., 2001). The Bradore Formation is conformably overlain by shallow-marine carbonate strata of the Forteau Formation and shallow-marine quartz arenite of the Hawke Bay Formation, which mark the end of the rift-drift transition (Lavoie et al., 2003; Dietrich et al., 2011). The sea-level low-stand ("Hawke Bay event", James et al., 1989) that generated the Hawke Bay Formation was followed by marine transgression and deposition of Port au Port and St. George group platformal carbonate strata (Fig. 2; Knight, 1997; Lavoie et al., 2003; Dietrich et al., 2011).

Passive margin sedimentation in western Newfoundland ceased during the onset of the Taconic orogenic cycle, which caused uplift due to a migrating peripheral bulge and resulted in an erosional surface known as the 'St. George Unconformity' (Cooper et al., 2001; Waldron et al., 2012). Middle Ordovician shelf subsidence was caused by the rapid emplacement of the Humber Arm allochthon onto the margin and provided accommodation space for limestone-dominated (Table Point Formation) and shale-dominated (Table Cove Formation; Waldron et al., 2012) units of the Table Head Group. Foreland basin subsidence was accompanied by syn-sedimentary extensional faulting, e.g., the Round Head Fault in the Port au Port area, which exposed between 500 m (Waldron et al., 2012) and 1000 m (Cooper et al, 2001) of platform stratigraphy in its scarp. Thick beds of Cape Cormorant Formation limestone conglomerate were deposited as scarp-related talus fans along the down-thrown hanging wall of the Round Head fault (Fig. 2; Cooper et al., 2001; Waldron et al., 2012). The succession of the Goose Tickle Group, including the Mainland Sandstone Formation, marks the transition from carbonate to clastic sedimentation in the immediate Round Head Fault hanging wall (Quinn, 1992; Waldron et al., 2012). The Goose Tickle Group formed as turbidite fans and infill of a starved, fault-bounded basin that was established in the Middle Ordovician (Quinn, 1992; Waldron et al., 2012).

Carbonate sedimentation in western Newfoundland was re-established during the Late Ordovician and preserved by Lourdes Formation strata (Long Point Group) that onlap the Taconic unconformity (Cooper et al., 2001; Waldron et al., 2012). Carbonate deposition transitioned to clastic sedimentation in the rapidly subsiding, post-Taconic foreland basin (Winterhouse and Mist Point formations; Waldron et al., 2012). The absence of Silurian strata implies that regional uplift and erosion occurred as a result of the Salinic orogenic event and now characterises the Salinic unconformity (Cooper et al., 2001; Dietrich et al., 2011; Waldron et al., 2012).

The upper Silurian-lowermost Devonian Clam Bank Formation consists of red and grey, marginal-marine clastic strata and minor carbonate rocks that represent the sedimentary fill as foreland basin sedimentation resumed during the Acadian orogeny (Waldron et al., 2012). The Emsian Red Island Road Formation that contains abundant rhyolite clasts of unknown origin and Early Devonian fossils and overlie the Clam Bank Formation (Cooper et al., 2001; Waldron et al., 2012). In the Port au Port Peninsula, Carboniferous successor basin strata include fluvial to lacustrine siltstone and shale, with regionally important marine evaporites of the Anguille, Codroy, and Barachois groups (Cooper et al., 2001; Waldron et al., 2012). Passive margin strata in the Port au Port area entered the oil window in the Early Devonian, resulting in peak petroleum generation and migration during the Acadian orogeny (Dietrich et al., 2011). Cambrian-Ordovician Green Point and Shallow Bay formation strata are the predominant source rocks in this region (Dietrich et al., 2011; Hinchey et al., 2015).

Allochthonous succession

The Humber Arm allochthon contains deep-water facies that were deposited on the continental slope and rise contemporaneously with the shallow-water facies along the autochthonous shelf (Fig. 2; Waldron et al., 2012). Thrust slices of the allochthonous succession were emplaced onto the shelf during the Taconic orogeny (Lavoie et al., 2003; Waldron et al., 2003). The Taconian thrusts and mélange belts were subsequently overprinted during the Acadian orogeny, e.g., as recognizable on the Port au Port peninsula (Waldron et al., 2012).

Pre-Taconic slope and rise facies of the Middle Cambrian to Middle Ordovician Cow Head Group were coeval with autochthonous rocks of the Port au Port and St. George groups and allochthonous Northern Head Group (Lavoie et al., 2003; Waldron et al, 2012). The Cow Head Group comprises proximal, limestone boulder conglomerate of the Shallow Bay Formation and distal black and green shale of the Green Point Formation (Cooper et al., 2001; Waldron et al, 2012; Hinchey et al., 2015). The basal Cambrian clastic unit that correlates with the Labrador Group on the shelf is not preserved in the Cow Head succession (Lavoie et al., 2003; Waldron et al., 2012). The distal slope and rise succession in the area of the Bay of Islands is the most complete of the tectonic slices and contains the Cambrian Summerside and Irishtown formations of the Curling Group, which are unconformably overlain by the middle Cambrian to Lower

Ordovician Cooks Brook and Middle Arm Point formations (Lavoie et al., 2003; Waldron et al., 2012). Foreland basin flysch deposits of the Lower Head and Eagle Island formations conformably overlie the Cow Head and Northern Head groups, respectively (Botsford, 1987; Waldron et al., 2012; Hinchey et al., 2015). The Summerside Formation consists of maroon and green slate that is interbedded with pale quartzose to arkosic meta-sandstone. The overlying Irishtown Formation contains interbedded, quartzose turbiditic sandstone, conglomerate, and locally pyrite-bearing slate (Lavoie et al., 2003; Waldron et al., 2012). Based on palynomorph and ichnological assemblages, the Cambrian Summerside and Irishtown formations correlate with the Cambrian Blow Me Down Brook Formation, which together represent the Curling Group, the deeper-water equivalent to the shallow-water clastic shelf succession of the Labrador Group (Lavoie et al., 2003; Waldron et al., 2012).

Cambrian and Ordovician clastic sandstone reservoir plays

Cambrian Hawke Bay Formation, Labrador Group

Quartz arenite units of the Hawke Bay Formation were deposited at the end of the rift-drift transition in a high-energy, shelf environment that was marked by a low-stand ("Hawke Bay Event"; Lavoie et al., 2003; Waldron et al., 2012). The Hawke Bay Formation (a.k.a. Degras Formation; e.g., Riley, 1962) is ~170 m-thick and exposed along an incomplete, 8 km-long section of cliff-bounded shoreline between Grand Jardin in the west and Marches Point in the east (Fig. 3; Knight and Boyce, 2014). Hawke Bay Formation beds strike WSW-ENE and dip to the NW and are locally cross-cut by WSW-ENE striking faults that dip to the SE (Knight and Boyce, 2014; this study). The normal faults have throws that range from a few centimetres to few metres (Knight and Boyce, 2014; this study). A ~5 cm thin carbonate conglomerate layer below a succession of Marches Point Formation shale and siltstone marks the top of the Hawke Bay Formation (Fig. 4a-b; Knight and Boyce, 2014; this study). The quartz arenites range from white, pink, green-grey, and red in colour and are glauconitic and micaceous, locally with interbedded siltstone and shale (Fig. 4c-h; Knight and Boyce, 2014; this study). The red colour locally may be secondary in nature and due to the proximity of the Carboniferous basin to the south beneath the St. George's Bay (Knight, 1983; Knight and Boyce, 2014). The Hawke Bay Formation was deposited in cleaning- and shoaling-upward parasequences that are 5 to 30 m-thick (Knight and Boyce, 2014). Dark-grey to black shale that is intercalated with bioturbated sandstone marks a recessive interval in the lowest exposed sequence just below the school at Degras/De Grau (Knight and Boyce, 2014). The lower recessive interval comprises poorly sorted, coarse-grained, locally granular to pebble, green and grey sandstone that contains strongly bioturbated horizons (Fig. 4e-f; Knight and Boyce, 2014). The Hawke Bay cliffs consist of tabular-stratified to cross-bedded, well sorted, very fine- to medium-grained, pale green to light grey and red quartz arenite, which locally are intercalated by green and red silty mudstone and micaceous siltstone and sandstone beds (Knight and Boyce, 2014). Sedimentary structures include ripple marks, planar and cross-lamination, and locally small hummocky cross stratification (Knight and Boyce, 2014; this study). The observed sandstone facies, sedimentary structures, and trace fossils are consistent with a high-energy, wave- and storm-dominated shelf and shoreline environment (Fürchtbauer, 1988; Knight and Boyce, 2014).

Clean quartz arenite units of the Hawke Bay Formation contain sections over 64 m-thick with up to 12.2% porosity (Port au Port #1 well) in the hanging wall of the Round Head Fault, a structure initially active as extensional fault during the Taconic orogeny and re-activated as a thrust fault during the Acadian orogeny (Cooper et al., 2001; Dietrich et al., 2011; Waldron et al., 2012). In the St. George's Bay A-36 well, the Hawke Bay arenites yield an average porosity of 10% over 31 m, but calculate wet on logs (Cooper et al., 2001). Probable structural traps are lateral sandstone pinchouts and sandstone channel-fills, as well as structural traps in fault blocks formed during extensional phase of the Round Head fault (Dietrich et al., 2011). In contrast, the Hawke Bay arenites in the footwall of the Round Head thrust are tight (~5% porosity), which is interpreted to be a result of higher post-Acadian burial depth (Cooper et al., 2001).

Cambrian Blow Me Down Brook Formation, Curling Group

Cambrian clastic sedimentary rocks crop out in the structurally highest sheet of the Humber Arm allochthon, but are roughly correlative with the Labrador Group clastic shelf succession (Palmer et al., 2001; Waldron et al., 2003). The Blow Me Down Brook Formation was originally defined by Lilly (1967) for the type locality. Easterly-derived, chromite-bearing Ordovician flysch units of western Newfoundland were previously included in the Blow Me Down Brook Formation and thought to have been deposited more distal to the autochthonous Goose Tickle Group (Quinn, 1985). Stevens (1970) recognized that the Blow Me Down Brook Formation sandstones were derived from silicic intrusive sources rich in microcline granite and sodic granophyre, ophiolites with gabbros, volcanic rocks, and chrome-spinel-bearing ultramafic rocks and sediments similar to older parts of the Curling Group, but interpreted them as easterly-derived flysch (Lindholm and Casey, 1989). However, Quinn (1985) re-interpreted the Blow Me Down Brook Formation as westerly-derived Precambrian or Cambrian succession of rift-related sandstones that now occur as a structurally high slice. An early Cambrian age is further indicated by palynomorphs (acritarch *Skiagia* sp.) that correlate with those found in the Irishtown and Summerside formations and the presence of the trace-fossil *Oldhamia antiqua* (Lindholm and

Casey, 1989; 1990; Palmer et al, 2001; Burden et al., 2005). Blow Me Down Brook Formation strata show strong similarities to the Cambrian Sellars Formation in the Bonne Bay area, which is described in detail by Quinn (1985) and the Cambrian Charny Formation of Québec (Hiscott, 2017; *pers. comm.*). Accordingly, in western Newfoundland the Blow Me Down Brook/Sellars Formation is essentially continuous along the eastern margin of the Bay of Islands complex, through the Pasadena map area to Blow Me Down Brook (Quinn, 1985), and possibly to the Two Guts Pond area in the eastern Port au Port Bay (Hicks and Owen, 2014; this study). A correlation of the Sellars and Blow Me Down Brook formations is further supported by the association of the Sellars Formation with the Cambrian Mitchells and Barters formations, which appear visually, compositionally, and texturally identical to the Summerside and Irishtown formations, respectively (Quinn, 1985). The Sellars Formation sandstones are commonly associated with Crouchers volcanic rocks, which possibly represent a similar rift-related origin as the sedimentary and volcanic rocks on Woods Island (Quinn, 1985). The provenance of the Sellars Formation indicates that they are derived from a Grenvillian basement plus sedimentary cover, which is consistent with the suggested provenance of the Blow Me Down Brook Formation (Quinn, 1985).

The Blow Me Down Brook Formation is well exposed at the type locality section around Blow Me Down Brook in the Bay of Islands (Candlelite Bay Inn area) and also along the southern western shore of Woods Island (Fig. 5; Quinn, 1985; Palmer et al., 2001; Lavoie et al., 2003; this study). Blow Me Down Brook Formation feldspathic and lithic sandstone, together with coeval fine- to coarse-grained facies of the Summerside and Irishtown formations, were deposited by episodic turbidity currents as submarine fans and/or other types of sedimentary gravity flows (Quinn, 1985; Palmer et al., 2001). The Woods Island succession is the most continuous and undisturbed section and to the east in stratigraphic contact with pillowed, massive, and brecciated mafic volcanic rocks of the Fox Island Group (Palmer et al., 2001; Hiscott, 2017; *pers. comm.*). This contact on Woods Island is likely the original base of the formation (Palmer et al., 2001). However, the stratigraphic contact between the mafic volcanic rocks and overlying basal red mudstones of the lowermost Blow Me Down Brook Formation is rarely preserved; in most other cases the contact is tectonic in nature (Quinn 1985; Palmer et al., 2001). Thick, competent sandstone beds on Woods Island are better preserved than the shaley facies of the formation, which are more likely to be incorporated into the mélange of the Humber Arm allochthon (Palmer et al., 2001).

The Blow Me Down Brook Formation consists of three main types of sandstones (Fig. 6-7; Sdst I, Sdst, II, and Sdst III). The lower unit consists of very thick (up to 3 to 5 m) amalgamated beds of graded, grey, medium- to very coarse-grained to pebbly sandstone (Fig. 6-7; 'Sdst I') with calcitic, locally patchy, alteration. Sandstone I is overlain by a 5 to 30 cm-thick bed of light grey, tight, medium- to coarse-grained sandstone (Fig. 6-7; 'Sdst II') with trough cross-lamination that is locally intercalated with dark grey shale and medium grey thin-bedded sandstone with convolute bedding (Fig. 6-7; 'Sh/Sdst II'). The shale unit is up to 1 m-thick, but is locally absent (Fig. 6-7). Where no shales are present, the light grey 'marker bed' is overlain by very thick (3 to 5 m), dark grey, very coarse-grained to granule to pebble sandstone (Fig. 6-7; 'Sdst III'). Sandstone units typically have scoured bases and contain red and white feldspar, milky quartz, detrital mica, and opaque minerals, as well as igneous and metamorphic lithic fragments and accessory heavy minerals. The upper dark grey sandstone unit contains more red-orange feldspar and the lower medium grey sandstone contains locally fissile dark-grey phosphatic mud/shale chips (Fig. 7; Palmer et al., 2001; this study). The latter features imply that the mud/shale chips were intraformational, but mostly removed by scouring and preserved as rip-up clasts in the sandstone units (Quinn, 1985; Palmer et al., 2001). The thick sandstone sequence is underlain by reddish to grey shale to siltstone that is intercalated with thin (1 to 4 cm) sandstone beds (Fig. 6-7), which locally are visible at the base of the cliffs on the shore under beach-forming boulders. Overall, Blow Me Down Brook Formation sandstone is texturally and compositionally immature indicating deep-sea submarine fan origin in a rift-drift transition environment (Palmer et al., 2001).

Sandstone reservoir plays in the Blow Me Down Brook Formation are based on secondary and fracture porosity, the latter locally improving reservoir permeability (Dietrich et al., 2011). Exhumed oil reservoirs with extensive sections of bituminous sandstone and shale occur in the Sluice Brook area (Burden et al., 2005; Dietrich et al., 2011). Bituminous Blow Me Down Brook strata also occur along shoreline outcrops of the Candlelite Bay Inn area (Fig. 7), Bay of Islands; Molly Ann Cove, and Rope Cove Head, shoreline west of the Lewis Hills; and on shoreline outcrops at Two Guts Pond, which are possible Blow Me Down Brook sandstones (Hicks and Owen, 2014; this study). The main traps are structural and related to fold and thrust structures (Dietrich et al., 2011). These reservoir plays have potential for enhanced porosity due to their occurrence adjacent to shaley allochthonous source beds, which potentially create secondary porosity due to the presence of organic matter that also can charge the porous Blow Me Down Brook Formation sandstones (Fürchtbauer, 1988; Burden et al, 2005). The Blow Me Down Brook sandstones in the Candlelite Bay Inn area are typically cross-cut by conjugate sets of faults, which may enhance the permeability of the formation and that locally are petrolifeorus (Fig. 7a and b_bottom left; Ferrill et al., 2009). In the area of the Candlelite Bay Inn a thick sequence of the sandstone and shale units (Sdst. I, Sdst. II, Sdst. III, and Sh. I) is overturned based on the stratigraphic succession of the characteristic sandstone and shale units and sedimentary structures (Fig. 7b). A detached tight fold hinge is observed in outcrop within the sandstone Sdst II that is commonly associated with shales (Fig. 7b). Similar tight detached fold hinges can also be synsedimentary slump structures (Calon, 2017, *pers. comm*.). Comparable overturned beds and fold structures are also described by Quinn (1985) for the Sellars Formation, Buchanan (2004) for the Blow Me Down Brook Formation at the same outcrop location, and Burden et al. (2006) in the geological map of the Bay of Islands area.

Ordovician Mainland Sandstone Formation, Goose Tickle Group

Middle Ordovician foreland flysch of the Goose Tickle Group are divided up into the Black Cove, Mainland Sandstone, and American Tickle formations (Waldron et al., 2012). Correlative units in the Humber Arm allochthon are the Lower Head and Eagle Island formations (Cooper et al., 2001; Waldron et al., 2012). The Mainland Sandstone Formation conformably overlies marine rocks of the Table Head Group, including Cape Cormorant Formation carbonate boulder conglomerate (Fig. 8a, c; Waldron et al., 2012). The Mainland Sandstone Formation is up to 622 m-thick and mostly consists of rhythmic sandstone and shale (Fig. 8a-h; Waldron et al., 2012; this study). Sandstone facies are normally graded and represent partial Bouma sequences, whereas the shale and finer-grained sandstone units locally contain graptolites (Waldron et al., 2012). The Mainland Sandstone formation is restricted to the west coast of the Port au Port peninsula and best exposed in the cliffs NE of Cape Cormorant, along the shoreline near the village of Mainland, and the cliffs at Crow Head (Figs. 3 and 8; Quinn, 1992). Rock units at the type locality are fine- to medium-grained with lesser amounts of thick-bedded, medium- to coarse-grained massive sandstone, locally with cross-bedding (Quinn, 1992; this study). Cross-bedded sandstone facies typically have scoured bases (Quinn, 1992; this study). Sedimentary structures include planar laminae (Fig. 8 b) with parting lineations, trough cross-laminae (Fig. 8d, g, h, l), ripple marks, soft-sediment deformational structures (Fig. 8e, f; small-scale slumping), carbonate concretions, and locally horizontal bioturbation. Further northeast, along the shoreline at Low Point, outcrops of the upper and most porous part of the formation are exposed (Fig. 8g-i; Quinn, 1992; this study). Porosity within the Mainland Formation Sandstone is locally significant, but does not exceed 10% (Quinn, 1992). The dominant type of porosity is secondary, and probably generated from the dissolution of feldspar and chloritized serpentinite grains by organic acids that were sourced from associated shale (Quinn, 1992; this study). The pores do not appear to be affected by compaction and retain their original shape (Quinn, 1992; this study). The uppermost sections of the Mainland Sandstone also display porosity as a result of calcite cement dissolution (Quinn et al., 1992). Generally, pores have poor interconnectivity resulting in poor permeability; however, bedding-parallel fracture porosity has the potential to enhance the permeability (Quinn, 1992; this study). Foreland basin sandstones are generally poorly sorted and compositionally and texturally immature, and therefore have low porosity (Morad et al., 2010; Dietrich et al., 2011). The secondary dissolution of chloritized serpentinite grains and feldspar can enhance initially low porosity if the pores have clay rims that prevent quartz cementation (Quinn, 1992; Bloch, 1994; Morad et al., 2010).

Ordovician Eagle Island Formation

Botsford (1987) assigned the name Eagle Island Formation to Ordovician flysch deposits that conformably overlie the Middle Arm Point Formation of the Northern Head Group, Humber Arm allochthon, Bay of Islands area. The Eagle Island Formation represents the easterly-derived strata that were deposited in advance of, and subsequently incorporated into, the westward moving allochthonous units (Stevens, 1970; Botsford, 1987). The >203 m-thick type section of the Eagle Island Formation is located at Middle Arm Point and displays a tectonic upper boundary that is commonly marked by the presence of mélange (Botsford, 1987). The contact between Eagle Island Formation and Middle Arm Point Formation is characterised by unit where sandstone chaotically is injected into Middle Arm Point shale (Botsford, 1987). This chaotic interval also contains turbiditic graded sandstone beds of <40 cm thickness (Botsford, 1987). Bedded sandstone, siltstone, and shale units overlie the basal chaotic shale-sandstone injection-interval; the latter is missing at Black Point (Fig. 3) in the East Bay, where bedded sandstone immediately overlies silicified shale units ("chert"; Fig. 9a) that are characteristic of the uppermost Middle Arm Point Formation (Botsford, 1987). The upper Middle Arm Point Formation also contains dolomite beds that are associated with red or green shale-dominated sequences (Fig. 9a-b; Botsford, 1987). The Eagle Island Formation consists of thick bedded, greenish, medium- to coarse-grained sandstone with, local accumulations of conglomerate (Fig. 9e-h), siltstone and grey shale (Fig. 9c; Botsford, 1987; this study). The lower part of the formation also contains red and green shale (Botsford, 1987). The faunal assemblage at the Black Point cliffs contains Ordovician graptolites (Botsford, 1987). The framework grains of the Eagle Island Formation sandstones at Black Point typically show a preferred orientation and locally are slightly cleaved (Fig. 9h). This contrasts with Blow Me Down Brook Formation strata that do not show any obvious preferred orientations in the Candlelite Bay or Bonne Bay areas (Sellars Formation; Quinn, 1985).

Two Guts Pond – Ordovician Eagle Island Formation or Cambrian Blow Me Down Brook Formation?

At Two Guts Pond on the eastern shore of Port au Port Bay, shoreline outcrop occurrences of grey, medium- to thick-bedded, very coarse-grained to pebbly sandstone with petroleum stains belong either to the Blow Me Down Brook Formation or Eagle Island Formation (Hicks and Owen, 2014). The framework grains are subangular to rounded and consist of red and white feldspar, quartz, and lithics (Fig. 10c-e). The sandstone beds are cross-cut by locally petroliferous fractures and also show bedding-parallel petroleum staining (Fig. 10a-b, f). The conjugate joint sets and type of weathering appear very similar to the very coarse-grained to pebbly sandstones of the Blow Me Down Brook Formation in the Candlelite Bay Inn area (Fig. 10g) and those reported by Quinn (1985) of the Sellars Formation in the Bonne Bay area (= Blow Me Down Brook Formation in the Humber Arm; Fig. 10h). Ongoing SEM-MLA studies may provide an opportunity to identify which formation (Eagle Island or Blow Me Down Brook) is exposed at Two Guts Pond.

Results

Sampling, methods, and quality control and quality assurance (QA/QC)

The focus of this research is the application of advanced micro-analytical imaging methodologies, such as scanning electron microscopy combined with mineral liberation analysis (SEM-MLA), to quantify the reservoir quality and porosity evolution of lower Paleozoic sandstones. Summer 2016 samples were collected during stratigraphic mapping along coastal and road outcrops in the Bay of Islands (Figs. 5; 11a-b) and Port au Port peninsula (Figs. 3; 11c).

Samples were taken from representative sandstone, siltstone, shale, and conglomerate units of the Cambrian Blow Me Down Brook Formation in the Candlelite Bay Inn area (Fig. 11b; BOI16_B1-17); Cambrian Hawke Bay Formation at Marches Point (Fig. 11c; PAP16_HB1-11) and De Grau (PAP16_HB12-18; Fig. 11c); Ordovician Mainland Sandstone Formation in the Mainland area, including the basal contact with the underlying Cape Cormorant Formation conglomerate (PAP16_CC1-3 and PAP16_MF1-12; Fig. 11c), Low Point (PAP16_MF13-16; Fig. 11c), and Crow Head (PAP16_MF17-22; Fig. 11c); Ordovician Eagle Island Formation in the Black Point area, including the basal contact with the Middle Arm Point Formation (BP16_E1-E7; Fig. 11c); and Blow Me Down Brook/Eagle Island Formation in Two Guts Pond area (TGP16_B/E1-2; Fig. 11c). Representative samples were collected across the stratigraphy from several beds in regular intervals from different outcrop locations. Furthermore, samples were obtained from the same stratigraphic horizons from laterally different locations. Polished thin-sections (23x46 mm) were prepared by Vancouver Petrographics and the cut-off blocks were returned.

Petrographic studies were conducted on samples of sandstone, siltstone, and shale. High resolution backscattered electron (BSE) images were obtained using a FEI Quanta 400 scanning electron microscope (SEM) at Memorial University, which is equipped with a Bruker energy dispersive x-ray (EDX) analytical system. Sandstone samples selected for SEM-MLA studies included those that were most representative of the studied lithology and, if present, contained petroliferous staining and/or visible porosity. Initial studies to set up the methodology concentrated on thin-sections from the Blow Me Down Brook Formation and selected samples from the Mainland Formation. Thin-section cut-off blocks of the Eagle Island Formation from Black Point and Blow Me Down Brook/ Eagle Island Formation from Two Guts Pond were analysed by SEM-MLA. Samples from the Hawke Bay Formation, the remaining samples from the Mainland Formation, and rocks within the Long Point M-16 core will be analysed in Summer 2017.

SEM-MLA: The SEM-MLA software was initially designed for mineral processing purposes and specified for mineral grain separates to study the degree of liberation of ore or industrial minerals (e.g., Fandrich et al., 2007, and references therein). Furthermore, SEM-MLA of thin-sections is commonly used for metamorphic petrology studies (e.g., A. Indares research group at the Department of Earth Sciences, Memorial University). Accordingly, methodologies related to petroleum geology require new development and to be efficiently applicable for reservoir quality and porosity evolution studies.

The SEM-MLA facility is located in the MAF-IIC Microanalysis Facility at Memorial University. Thin-sections were carbon-coated and analysed using the FEI MLA 650 FEG Scanning Electron Microscope (SEM) that is equipped with Mineral Liberation Analyser (MLA) software developed at the Julius Kruttschnitt Mineral Research Centre (JKTech), Queensland, Australia. The filament was set to 25 kV and a beam current of 10nA with an operating distance of 13.5 mm between sample and detector was used to obtain high-resolution SEM-MLA maps of each thin-section. The sample is configured in the SEM using backscattered electron (BSE) mode that creates detailed high-resolution grey-scale images. The SEM-MLA software is able to recognize the mineral species by using Energy Dispersive X-ray Spectroscopy (EDX) spot analysis and creates mineral-specific elemental spectra that are compared with those in an existing user-defined reference library. The SEM-MLA maps are created in XBSE mode (extended BSE liberation analysis) by acquiring an EDX-ray spot analyses every 10-12 pixels over the entire thin-section. The master SEM-MLA library contains numerous minerals that can be used to create a project-oriented, user-specific mineral library. The mineral spectra are based on the elements present in the mineral and their relative concentrations; however, it cannot characterise the crystallography of the mineral. For grain mounds, the SEM-MLA software defines a particle as one individual mineral grain, whereas for analysed thin-sections, a particle is a frame of 1.5 mm x 1.5 mm @ 3µm/pixels.

The SEM-MLA software creates digital false-colour maps of the thin-section, which can be analysed and processed after the MLA runs are completed. The user can define the colour for each mineral; colours used for this study are shown in Figure 12. After post-processing review, the data and digital maps for each sample were re-calculated using standard procedures, such as a 70%-fit threshold matching parameter. Unknown mineral facies can further be specified and added to the library after a SEM-MLA run is completed, which reduces the %unknowns generally to <0.1% (Wilton et al., 2016). By running a specifically defined script, unkowns smaller than ~10-20 pixel were converted to the host mineral, as they represent 'noise' in the obtained mineral spectra, whereby noise represents grain boundaries, unresolvable mixed signals, cracks, etc. BSE grey scales of <40 characterise the epoxy in which the rock sample is mounted in the thin-section, and therefore, represents epoxy-filled porosity in the rock. A porosity script was applied to convert the mapped epoxy/background into porosity. Because of the high resolution macro-, meso-, and microspores, e.g., porosity between layers of sheet minerals, as well as fracture porosity and secondary porosity can be recognized and quantified. Fractures were chosen to be converted to porosity as they may represent possible conduits for hydrocarbons. If the margins of a thin-section were too thin and/or friable, the margins of the created digital MLA maps were cleaned-up by removing the friable marginal particles before the analysed data sets were created.

After the post-processing of the SEM-MLA maps, a database containing all images and statistical information is created using the SEM-MLA software. These databases can be exported and imported to the Dataview software, which produces Excel tables with all created data results (mineral distributions based on area (area% and micron) and weight%, number of mineral/particle counts, and element distributions. Weight% data is a calculated result based on the given density of the mineral in the library and does not represent true weight%. Therefore, it should not be used for the interpretation of data. Furthermore, the Dataview software can create a variety of visual data analysis. For this study, however, the created Excel tables were imported to the software Gigaset Aabel_3, a program for statistical and exploratory data analysis and visualisation and diagrams were produced accordingly. In the following Results section and in the figures, the given data % represent area% of a certain mineral in the thin-section.

Results and identification of potential problems - quality control and quality assurance (QA/QC)

Blow Me Down Brook Formation: Samples from the Blow Me Down Brook Formation were collected from the Candlelite Bay Inn area (Fig. 11a-b) covering sequences vertically across the stratigraphy, including the basal coarse-grained sandstone (Sdst I), the overlying light grey medium-grained sandstone (Sdst II), and the upper very coarse-grained to pebbly sandstone (Sdst III), as well as sandstone beds that are intercalated with shales (Sh-sdst II) localy occurring between the two thick coarse-grained sandstone packages (Figs. 6-7).

The thick basal sandstones (Sdst I; Figs. 6, 7, 13) of the Blow Me Down Brook Formation consist of 56.4 to 59.9% quartz, 20.5 to 27.1% feldspars (K-feldspar and plagioclase combined), 0.03 to 4.8 carbonates (calcite, dolomite, ankerite, siderite combined), 12.1 to 15.3% clays *sensu latu* (chlorite, kaolinite, illite, glauconite, clinochlore), and 0.2 to 0.9% organic matter with porosities ranging from 0.1 to 0.7% (Fig. 13). Furthermore, these basal sandstones contain between 0.1 to 0.7% phosphatized shale fragments (Figs. 7, 13).

The light grey medium-grained sandstone samples (Sdst II) overlying the basal sandstone (Sdst I) contain 51.1 to 60.2% quartz, 23.9 to 28.8% feldspars (K-feldspar and plagioclase combined), 0.05 to 0.4 carbonates (calcite, dolomite, ankerite, siderite combined), 12.8 to 19.7% clays *sensu latu* (chlorite, kaolinite, illite, glauconite, clinochlore), and 0.3 to 0.6% organic matter with porosities ranging from 0.2 to 0.6% (Figs. 6, 7, 14).

The upper dark grey very coarse-grained to pebbly sandstone samples (Sdst III) are less quartzose with 49.9 to 52.6% quartz, 22.0 to 25.7% feldspars (K-feldspar and plagioclase combined), 0.002 to 0.7 carbonates (calcite, dolomite, ankerite, siderite combined), and have higher clay contents with 18.4 to 23.0% clays *sensu latu* (chlorite, kaolinite, illite, glauconite, clinochlore), and 0.3 to 0.6% organic matter with porosities ranging from 0.2 to 0.6% (Figs. 6, 7, 15). Accordingly, the main types of the Blow Me Down Brook Formation sandstones fall within the feldspathic to lithic feldspathic arenite fields (wacke, if >15% clay content; Folk, 1980).

Sandstones that occur between the thick sandstone units (Sdst I and III) and are intercalated with shale of variable thickness and the light-grey weathering sandstone (Sdst II; Figs. 6-7, 16) range from very fine-grained to medium grained. They are either strongly calcite-cemented (Fig. 16_B11) or have abundant clay contents (predominantly illite; Fig. 16_B12 and B15). Quartz contents range between 21.8 and 35.2%, feldspars (K-feldspar and plagioclase combined) between 13.3 and 36.3%, carbonates (calcite, dolomite, ankerite, siderite combined) between 0.001 and 23.6%, and contain 14.2 to 44.4% clays *sensu latu* (chlorite, kaolinite, illite, glauconite, clinochlore), and 0.9 to 2.0% organic matter with porosities ranging from 0.1 to 2.1%. It is noticeable that the samples B12 and B15 have high clay contents and only negligible carbonate cements and especially the friable illite-rich sample B15 also has a higher porosity (2.1%) than the other samples (Fig. 16).

Carbonates (cement and veinlets) are more common in the basal sandstone (Sdst I) than in the overlying sandstones (Sdst II and III) and occur predominantly in veinlets, commonly conjugate sets of joints, with calcite diffusely penetrating the surrounding host rock, indicating that porosity was present pre-calcite cement precipitation. Calcite commonly fills extensional veins, fractures (Figs. 6, 7, 13, 17). For all sandstone types, quartz occurs as monocrystalline detrital quartz and polycrystalline lithic metamorphic characterised by subgrains with extinction in different crystallographic directions, and as part of lithic igneous fragments that contain quartz, microcline, albite, ±accessory phases (Figs. 18, 20). K-feldspars consist of orthoclase and microcline with its characteristic polysynthetic tartan twinning (Fig. 17_TL-x micrograph, middle right). Plagioclase occurs as pure albite, commonly untwinned, and polysynthetically twinned plagioclase with ranging from oliglase to andesine, minor anorthite in composition (based on the extinction angles of the polysynthetic twins). K-feldspars are commonly perthitic and/or display patchy albite alteration (Figs. 17-20). Locally, the K-feldspars show paragenetically later-stage patchy calcite-alteration (post albite alteration). Accessory minerals are detrital micas (muscovite and biotite), garnet, apatite, zircon (detrital grains or igneous zircons within lithic fragments), monazite, thorite (one grain up to 0.5 mm, samble B10 Sdst II), Y-xenotime, titanite, rutile, ilmenite, ilmenorutile, or intergrown mixed versions of these Ti-minerals, Fe-ox (hematite and/or magnetite), pyrite (framboidal or sub- to euhedral), chalcopyrite, and sphalerite. Heavy minerals are locally enriched in fine layers marking laminations (e.g., Fig. 20_BOI16_B12). Furthermore, they contain between 0.00006 and 0.003 % Mg-rich chromite that is locally associated with clinochlore (Fig. 19e-f). Glauconite occurs as oval to irregular shaped grains (Fig. 19g-h). Barite is present as grains or diagenetic rims around quartz and/or K-feldspars or as crack-infill. Phosphatized shale chips can occur up to 5 cm in size and commonly are oval or elongated grains consisting predominantly of apatite and minor, feldspars, quartz, micas, and organic matter (Fig. 18).

Mainland Sandstone Formation: Samples from the Mainland Sandstone Formation were collected from coastal outcrops on the Port au Port peninsula, from Cape Cormorant to Mainland, Low Point, and Crow Head (Fig. 11c). The carbonate conglomerate of the Cape Cormorant Formation that marks the lower contact of the Mainland Sandstone Formation was also sampled and run with the SEM-MLA to test whether the thin-section methodology is also applicable for carbonatic rocks. The master library contains numerous carbonate spectra that can be applied to detect the varying carbonate species. If an unknown carbonate would be present it would be mapped as 'unknown' and could be subsequently added to the user specific library. If a, e.g., a calcite crystal is enclosed by calcitic cement, the SEM-MLA software would not distinguish between mineral and cement. However, if for example, the calcite crystal contains trace amounts of Mn (or other element), and the cement is pure calcite, a script could be applied to distinguish between the two calcitic phases mineral and cement.

The sample (PAP16_CC3) of the Cape Conglomerate Formation was collected from a pebble to granule conglomerate immediately stratigraphically underlying the massive boulder conglomerate bed of the Cape Cormorant Formation. It contains 11.3% quartz, 2.1% feldspars (K-feldspar and plagioclase combined), 68.5% carbonates (28.4% calcite, 33.43% dolomite, 6.7% ankerite), and contains 0.2% clays *sensu latu* (chlorite, kaolinite, illite, glauconite, clinochlore combined), and 1.0% organic matter with a porosity of 0.01. A calcite-quartz-mix (50:50%) was added to the library for the carbonatic samples, as they commonly contain grains with a core of quartz with a rim of a mixed calcite and quartz. The stratigraphically overlying sample PAP16_MF10 consists of 28.0% quartz, 21.6% feldspars (K-feldspar and plagioclase combined), 10.0% carbonates (5.8% calcite, 2.2% dolomite, 2.0% ankerite), and contains 33.9% clays *sensu latu* (chlorite, kaolinite, illite, glauconite, clinochlore combined), and 3.8% organic matter with a porosity of 0.6. Sample PAP16_MF12 is a calcarenite intercalated with the shales and siltstones of the Mainland Sandstone Formation. It has a quartz content of 3.3%, feldspars of 1.7%, 88.8% of carbonates (45.3% calcite, 36.8% dolomite, 6.7% ankerite, 0.001% siderite), and contains 1.0% clays *sensu latu* (chlorite, kaolinite, illite, glauconite, clinochlore combined), and 1.4% organic matter with a porosity of 0.1 (Fig. 17). The Mainland Sandstone Formation samples from the Low Point and Crow Head locations are more quartzose and contain less carbonates, with quartz contents ranging between 32.5 and 63.1%, feldspars (K-feldspar and plagioclase combined) between 8.9 and 22.7%, carbonates (calcite, dolomite, ankerite, siderite combined), contain 7.8 to 30.9% clays *sensu latu* (chlorite, kaolinite, illite, glauconite, clinochlore), and 1.5 to 3.7% organic matter with porosities ranging from 0.6 to 9.8% (Fig. 23). It is noticeable that the sample PAP16_MF14 (Low Point) contains significantly more quartz, less feldspars, and has a higher porosity of 9.8%, which is consistent with porosity values report by Quinn (1992) for the Mainland Sandstone Formation in the Low Point area. Porosity is predominantly secondary in nature and a result of the dissolution of K-feldspar (Fig. 23) and of chloritized serpentinite grains (Fig. 23).

The Mainland Sandstone Formation sandstone contain between 0.0004 and 0.04% Mg-rich chromite with an average of 0.02 (Fig. 24), which is considerably higher than the chromite contents of the Blow Me Down Brook Formation (average of 0.001% chromite). The carbonate conglomerate bed of the Cape Cormorant Formation does not contain any chromite, which also is anticipated, as the thick beds of the Cape Cormorant Formation carbonate conglomerates were formed as westerly-derived talus fan deposits containing carbonatic shelf debris. The Mainland Sandstone Formation sandstones appear to contain recycled Blow Me Down Brook Formation sandstones, since the detrital components are similar in appearance, with mono- and polycrystalline quartz, igneous lithic fragments, and a similar suite of feldspars, including microcline (Fig. 23).

Mineral grouping: rigid, ductile, matrix, and pores: Another useful application of the SEM-MLA software is the mineral grouping tool. This grouping tools allows to group minerals according to the chosen research aspect. In this study, rigid, ductile, and matrix minerals accordingly have been grouped together, and maps created using this grouping and with the porosity remaining (Figs. 25-30). The SEM-MLA maps using the grouping allows to visually determine where in the thin-section/ the rock the individual rigid, ductile, and matrix components are located and their relationships to each other, and where in this framework the porosity occurs. Rigid components were classified based on their hardness, crystal habit, and alteration behaviour; e.g., K-feldspars were classified as rigid component, whereas albite and plagioclase were grouped as ductile, as they show ductile deformation behaviour in thin-section. Additionally, the data is also provided as data tables and therefore, can be used for statistical investigations.

The basal Blow Me Down Brook Formation sandstones (Sdst I) have 64.2 to 68.7% rigid components, 12.6 to 21.0% ductile components, and a matrix of 14.2 to 19.4% with porosity value of 0.1 to 0.7%, as given earlier already (Fig. 25). The stratigraphically overlying sandstone (Sdst II) contains 56.7 to 68.8% rigid and 16.4 to 21.9% ductile components, and matrix contributions between 13.2 and 20.8% with porosities of 0.2 to 0.6% (Fig. 26). The dark grey very coarse-grained to pebbly upper sandstone (Sdst III) has 60.0 to 63.3% rigid grains, 15.2 to 16.0% ductile components, 18.9 to 23.7% matrix, and porosities between 0.9 to 1.9% (Fig. 27). The sandstone that are intercalated with shales contain between 32.6% and 45.3% rigid, 17.4 to 27.4% ductile, and 27.4 to 45.6% matrix components with porosities between 0.1 and 2.1% (Fig. 28). The Cape Cormorant Formation conglomerate contains 12.4% rigid grains, 1.1% ductile grains, a matrix of 86.4%, and a porosity of 0.01%. The Mainland Sandstone Formation sandstones have rigid components between 4.4 and 68.2%, ductile components between 1.1 and 20.1%, matrix between 16.1 and 94.1% and porosities between 0.01 and 9.1% (Figs. 29 and 30).

Potential problems

Fe-Mg garnet versus Fe-Mg chlorite: The SEM-MLA acquires mineral spectra every 10-12 pixel over the whole area of the thin-sections. The acquisition of a mineral spectrum is based on the elements present in the mineral and their relative concentrations. This may create problems, because the crystallography of the mineral cannot be determined by SEM-MLA and in rare cases where the BSE-grey shade and the mineral spectra are extremely similar, minerals can be falsely identified. For example, the digital MLA maps of samples containing detrital Fe-Mg-garnet as accessory mineral and Fe-Mg-chlorite may falsely identify the Fe-Mg-garnet as Fe-Mg-chlorite and vice versa. Even though the crystallography (i.e., crystal class, habit) of those two minerals are significantly different, they are very similar in their BSE-grey shades and their mineral spectra. The different habit can easily be seen in the SEM-BSE image, as the garnet often occur as fragments of subhedral crystals with the, for garnet characteristic, conchoidal fractures, whereas chlorite is a fine-grained sheet silicate filling matrix space. Since the garnet fragments commonly are larger in size than the chlorite in the matrix, a script was applied to convert matrix chlorite that was falsely mapped as garnet into chlorite. Furthermore, for quality control and assurance measures, the SEM-MLA maps were compared to the SEM-BSE images and the remaining falsely identified garnets and chlorites manually corrected accordingly in the SEM-MLA software.

Porosity: The porosity script used in the SEM-MLA laboratory is an automated script that converts mapped background (i.e., epoxy) into porosity. Because of its automation, it cannot distinguish between plucked grains and moldic porosity. Plucked grains are a result of polishing and most commonly occur close to the edges of the polished thin-section (Pittman, 1991). Accordingly, for quality control and quality assurance pore space with euhedral mineral shapes when close to the margins of the thin-sections were manually converted back to background, This procedure does introduce a human bias; however, it was chosen to apply a conservative approach to avoid calculating falsely high porosity. The porosity script is still under development to further enhance the applicability of SEM-MLA porosity values for reservoir quality determinations. However, preliminary results are promising and presented in the following section.

Interpretation, summary, and outlook

The initial goal of the reservoir quality and porosity evolution project was to test and further develop automated SEM-MLA methodologies on thin-sections. For this testing phase, predominantly texturally and compositionally immature sandstones, but also carbonate conglomerate and calcarenite, were investigated.

Provenance

Based on the SEM-MLA mineralogical results, the Blow Me Down Brook Formation has igneous, metamorphic, and sedimentary provenance components that are consistent with local Grenvillian provenance (e.g., Quinn, 1985; Palmer et al., 2001; Burden et al., 2005). Microcline is characteristic of igneous provenance and occurs either as single grains or as part of a lithic fragment with quartz ± albite. Garnet crystals occur as angular to subangular fragments and are noticeably abundant in the rift-related Blow Me Down Brook sandstones, further indicating a proximal Grenvillian provenance. Furthermore, the SEM-MLA detected chromite not only in the Goose Tickle Group, where it is an expected accessory mineral, but also in the Blow Me Down Brook Formation. As the latter is Cambrian in age, the chromite cannot be derived from the Ordovician ophiolites, as it is suggested for the Ordovician flysch deposits. However, the Blow Me Down Brook Formation sandstones conformably overlie the Fox Island Group mafic volcanic rocks. Rift-related mafic volcanic rocks such as the Fox Island Group are known to be chromite-bearing (e.g, Meffre et al., 2004). *In-situ* trace element geochemistry studies of chromite and other key accessory minerals are planned in 2017 to complement the SEM-MLA studies. These *in-situ* data are expected to distinguish provenance components of the Cambrian rift-related Blow Me Down Brook Formation and Ordovician foreland basin flysch deposits. Detailed interpretation regarding source-to-sink systems of the Laurentian passive margin will be undertaken, once all samples were processed by SEM-MLA and will be report in a subsequent report.

The Ordovician Mainland Sandstone Formation contains microcline as singular grains or as part of lithic grains, but in lesser amounts than that of the Blow Me Down Brook Formation. Garnet is rare and significantly less abundant in Ordovician strata than in Cambrian rocks. This suggests that the Ordovician sandstones were in part recycled from the Blow Me Down Brook Formation (e.g., Quinn, 1992). Furthermore, the higher chromite content in the flysch deposits is expected, because of the detritus contributions of the easterly-derived ophiolite complexes to the Mainland Sandstone Formation sandstones.

SEM/MLA methodology

SEM-MLA runs were undertaken on the cut-offs blocks of thin-sections of the Eagle Island Formation sandstones to test whether the effect of plucking of grains during the polishing process can be reduced. Plucking of grains creates artificial porosity, which should not be included in the porosity calculations. For these tests, the blocks were carbon-coated and, since they are not polished, analysed in a low vacuum setting. Post-MLA sample processing is still ongoing, but initial results show potential for an application for future studies, e.g., studies on rock cuttings obtained from wells. For quality control and quality assurance, polished thin-sections of the same cut-off samples will further be analysed using SEM-MLA. Therefore, these test runs provide an excellent opportunity to compare the functionality of high vacuum studies on polished thin-sections versus low vacuum studies on the cut-off blocks. If the latter is of satisfactory quality (as it currently appears to be), it would be a method especially useful for petroleum industry, since it is a non-destructive methodology that can be applied on well rock cuttings.

Summary

In summary, the high resolution digital maps of the scanned thin-section obtained by using SEM-MLA methodologies, produces and provides detailed information concerning modal mineralogy, the effective porosity, grain-composition, -size, and -shape, and sorting of a rock sample. Furthermore, dissolution/ precipitation reactions of the minerals in the rock sample are recognisable in the digital SEM-MLA maps and therefore, this method provides an opportunity to study the porosity (primary and secondary) as well as reservoir quality evolution and additionally, provides information regarding provenance of the sandstones. Future studies will address the further development of the thin-section SEM-MLA methodology and especially of the porosity script for best possible research results. Further studies on the application of the porosity script on rock samples (e.g., thin-section cut-offs and/or rock cuttings) are ongoing and may have the potential to be applicable for industrial purposes.

Acknowledgements

The authors appreciate the financial support by the Petroleum Exploration Enhancement Program (PEEP). Kind support was also provided by Dylan Goudie and Dave Grant at the CREAIT SEM-MLA Laboratory and Larry Hicks and Karen Waterman at the Energy Branch of the Department of Natural Resources of Newfoundland and Labrador.

References

Bloch, S., 1994, Secondary porosity in sandstones: significance, origin, relationship to subaerial unconformities, and effect on predrill reservoir quality prediction, *in* M. D. Wilson, ed., Reservoir quality assessment and prediction in clastic rocks: SEPM Short Course 30, p. 137–160.

Botsford, J., 1987, Stratigraphy and sedimentology of Cambro-Ordovician deep water sediments, Bay of Islands, western Newfoundland, Ph.D. Thesis, Memorial University of Newfoundland, St. John's, NL.

Buchanan, C.R., 2004, Structural architecture and evolution of the Humber Arm allochthon, French Man's Cove – York Harbour, Bay of Islands, Newfoundland, MSc Thesis, Memorial University of Newfoundland, St. John's, NL.

Burden, E.T., Gillis, E. and French, E., 2005, Tectonostratigraphy of an exhumed Blow Me Down Brook Formation hydrocarbon reservoir, Sluice Brook, Western Newfoundland. *In* Current Research, Newfoundland and Labrador Department of Natural Resources, Geological Survey, Report 05-1, pages 63-71.

Burden, E.T., Calon, T., and Buchanan, C.R., 2006, Geology of part of the Humber Arm allochthon, Lark Harbour – Serpentine Lake area (NTS 12G/1, 12G/2, 12B/15, 12B/16), western Newfoundland, Government of Newfoundland and Labrador Department of Natural Resources, Geological Survey, Map 2006-03, Open File NFLD 2926.

Conliffe, J., Burden, E.T., and Wilton, D.H.C., 2017, The use of integrated fluid inclusion studies for constraining petroleum charge history at Parsons Pond, Western Newfoundland, Canada, Minerals 2017, 7, 39; doi:10.3390/min7030039.

Cooper, M., Weissenberger, J., Knight, I., Hostad, D., Gillespie, D., Williams, H., Burden, E., Porter-Chaudhry, J., Rae, D., and Clark, E., 2001, Basin evolution in western Newfoundland: New insights from hydrocarbon evolution: AAPG Bulletin, v. 85, p. 393-418.

Dietrich, J., Lavoie, D., Hannigan, P., Pinet, N., Castonguay, S., Giles, P., and Hamblin, A., 2011, Geological setting and resource potential of conventional petroleum plays in Paleozoic basins in eastern Canada, Bulletin of Canadian Petroleum Geology, vol. 59, 1, p. 54-84.

Fandrich, R., Gu, Y., Burrows, D., and Moeller, K., 2007, Modern SEM-based mineral liberation analysis, International Journal of Mineral Processing, v. 84, p. 310–320.

Ferrill, D.A., Morris, A.P., and McGinnis, R.N., Crossing conjugate normal faults in field exposures and seismic data, AAPG Bulletin, v. 93, no. 11, p. 1471– 1488.

Füchtbauer, H., Heling, D., Müller, G., Richter, D.K., Schmincke, H.-U., Schneider, H.-J., Valeton, I., Walther, H.W., and Wolf, M., 1988, Sedimente und Sedimentgesteine-Sedimentpetrologie, Teil II: Stuttgart, p. 1–1141.

Hicks, L. and Owens, J., 2014, The history of petroleum exploration in western Newfoundland, Government of Newfoundland and Labrador, Department of Natural Resources. Available Online: http://www.nr.gov.nl.ca/nr/energy/pdf/history_petroleum_exploration_western_nl.pdf.

Hinchey, A., Knight, I., Kilfoil, G., and Hicks, L., 2015, Geological overview and hydrocarbon potential of Cambrian-Ordovician strata of the outer Humber Zone, western Newfoundland, Current Research - Geological Survey of Canada, 15-1, Newfoundland and Labrador Department of Natural Resources, p. 143-171.

Hogg, J.R. and Enachescu, M.E., 2015, Petroleum Potential and Exploration Framework of Western Newfoundland Sedimentary Basins. DNR Report Number RPT-212:2015.

James, N.P., Stevens, R.K., Barnes, C.R. and Knight, I., 1989, Evolution of a lower Paleozoic continental-margin carbonate platform, northern Canadian Appalachians. *In* Controls on Carbonate Platform and Basin Development. Edited by P.D. Crevello, J.J. Wilson, J.F. Sarg and J.F. Read. Special Publication Society of Economic Paleontologists and Mineralogists, v. 44, p. 123-146.

Knight, I., 1997, Geology of Cambro-Ordovician Carbonate Shelf and Coeval Off-Shelf Rocks, Southwest of Corner Brook, Western Newfoundland, *In* Current Research. Newfoundland Department of Natural Resources, Report 97-1, pages 211-235.

Knight, I. and Boyce, W.D., 2014, Lithostratigraphy and correlation of measured sections, Middle Cambrian Hawke Bay Formation, western Port Au Port Peninsula, Government of Newfoundland and Labrador, Department of Natural Resources, Geological Survey, Open File 012B/06/0626.

Lavoie, D., Burden, E., and Lebel, D., 2003, Stratigraphic framework for the Cambrian-Ordovician rift and passive margin successions from southern Quebec to western Newfoundland, Canadian Journal of Earth Sciences, v. 40, p. 177-205.

Lilly, J.D., 1967, Some notes on stratigraphy and structural style in central West Newfoundland, Geological Association of Canada, Special Paper 4, p. 201-211.

Lindholm, R. S., and Casey, J. F., 1989, Regional significance of the Blow Me Down Brook Formation, western Newfoundland: New fossil evidence for an Early Cambrian age: Geological Society of America Bulletin, v. 101, p. 1-13.

Lindholm, R.M. and Casey, J.F., 1990, The distribution and possible biostratigraphic significance of the ichnogenus Oldhamia in the shales of the Blow Me Down Brook Formation, western Newfoundland, Canadian Journal of Earth Sciences, .27, p. 1270-1287.

Meffre, S., Direen, N.G., Crawford, A.J., Kamenetskya, V., 2004, Mafic volcanic rocks on King Island, Tasmania: evidence for 579 Ma break-up in east Gondwana, Precambrian Research, v. 135, p. 177–191.

Morad, S., Al-Ramadan, K., Ketzer, J.M., De Ros, L.F., 2010, The impact of diagenesis on the heterogeneity of sandstone reservoirs: A review of the role of depositional facies and sequence stratigraphy, AAPG Bulletin, v. 94, no. 8, p. 1267– 1309.

Palmer, S.E., Burden, E., and Waldron, J.W.F., 2001, Stratigraphy of the Curling Group

(Cambrian), Humber Arm Allochthon, Bay of Islands. *In* Current research, Newfoundland Department of Mines and Energy, Geological Survey Report 2001-1, pp. 105–112.

Quinn, L., 1985, The Humber Arm allochthon at South Arm, Bonne Bay, with extensions in the Lomond area, west Newfoundland, Phd Thesis, Memorial University of Newfoundland.

Quinn, L., 1992, Diagenesis Of The GooseTickle Group, Western Newfoundland, EL# 92-103-01-EG.

Riley, G.C., 1962, Stephenville map-area, Newfoundland, Geological Survey of Canada, Memoir 323, 72 p.

Stevens, R.K., 1970, Cambro-Ordovician flysch sedimentation and tectonics in west Newfoundland and their possible bearing on a Proto-Atlantic Ocean. *In* Flysch sedimentology in North America. Edited by J. Lajoie, Geological Association of Canada, Special Paper 7, p. 165-177.

Stockmal, G.S. and Waldron, J.W.F., 1990, Structure of the Appalachian deformation front in western Newfoundland: Implications of multichannel seismic reflection data. Geology, v. 18, p. 765-768.

van Staal, C.R. and Barr, S.M., 2011, Lithospheric architecture and tectonic evolution of the Canadian Appalachians and associated Atlantic margin In: Percival JA, Cook FA, Clowes RM (eds) Chapter 2 Tectonic Styles in Canada: the LITHOPROBE Perspective. Geological Association of Canada, p. 3-55.

Waldron, J. W. F., Henry, A. D., Bradley, J. C., and Palmer, S. E., 2003, Development of a folded thrust stack: Humber Arm Allochthon, Bay of Islands, Newfoundland, Appalachians, Canadian Journal of Earth Sciences, v. 40, p. 237-253.

Waldron, J.W.F., Hicks, L. and White, S.E., 2012, Stratigraphy, tectonics and petroleum potential of the deformed Laurentian margin and foreland basins in western Newfoundland. Geological Association of Canada–Mineralogical Association of Canada Joint Annual Meeting, Field Trip Guidebook B3. Newfoundland and Labrador Department of Natural Resources, Geological Survey, Open File NFLD/3172, 131 pages.

Williams, H., 1979, Appalachian Orogen in Canada: Canadian Journal of Earth Sciences, v. 16, p. 792-807.

Williams, H., 1995, Geology of the Appalachian-Caledonian Orogen in Canada and Greenland: Geology of Canada, v. 6.

Wilton, D.H.C, Feely, M., Carter, J., Costanzo, A., and Hunt, J., 2016, The application of automated SEM-based identification of detrital and diagenetic mineral phases in offshore cuttings from the Labrador Sea – Looking for the source, OTC-27380-MS, p. 1-10.

Zagorevski, A., van Staal, C.R., Rogers, N., McNicoll, V.J., and Pollock, J., 2010, Middle Cambrian to Ordovician arc-backarc development on the leading edge of Ganderia, Newfoundland Appalachians, Geological Society of America Memoirs, v .206, p. 367-396. doi: 10.1130/2010.1206(16).

Figures

Fig. 1

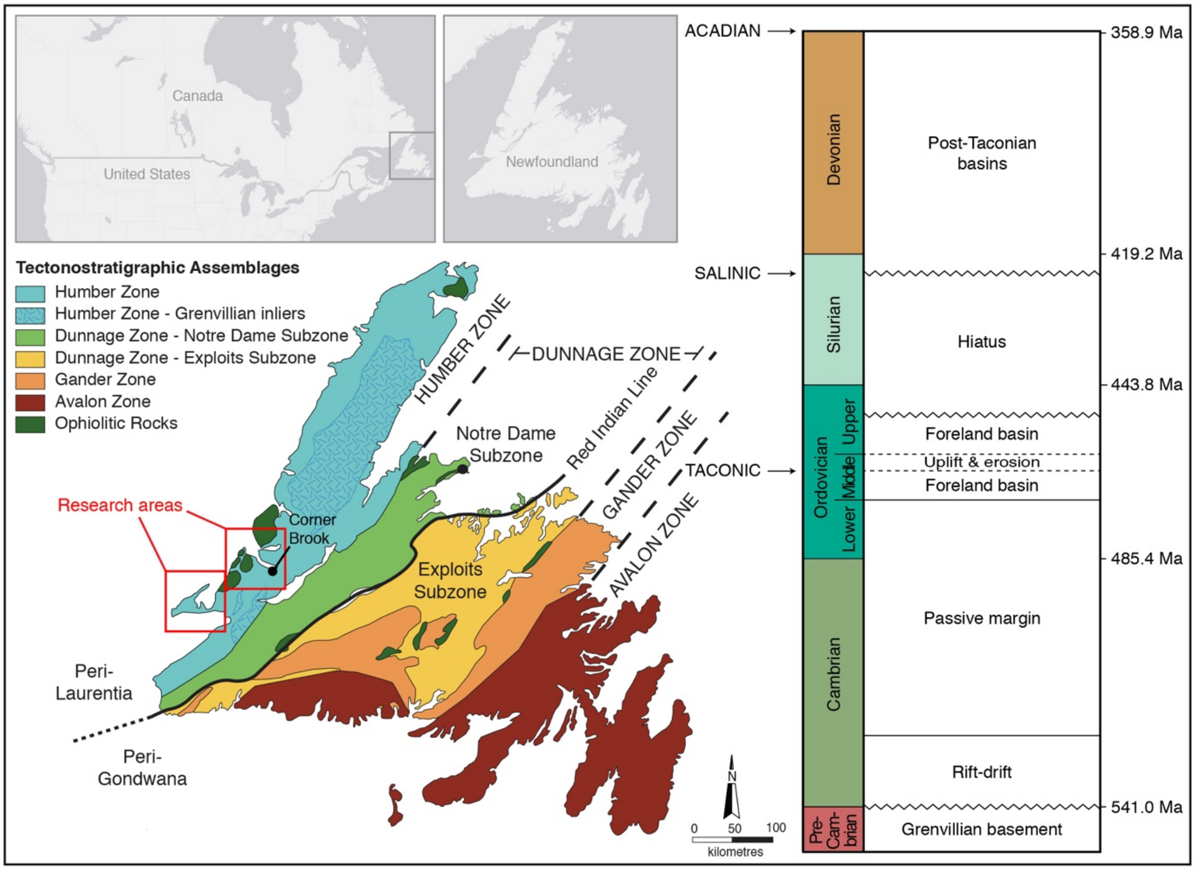

Fig. 1

Tectonostratigraphic assemblages with the main zones of the Newfoundland Appalachians (Avalon, Gander, Dunnage, and Humber zones). Modified after Lavoie et al. 2003, Hogg and Enachescu, 2015; Lode et al. 2016, and references therein. Numbers in Million years (Ma) after Cohen, K.M., Finney, S.C., Gibbard, P.L., & Fan, J.-X. (2013; updated) The ICS Chronostratigraphic Chart. Episodes 36: 199-204. http://www.stratigraphy.org/ICSchart/ChronostratChart2017-02.pdf

Fig. 2

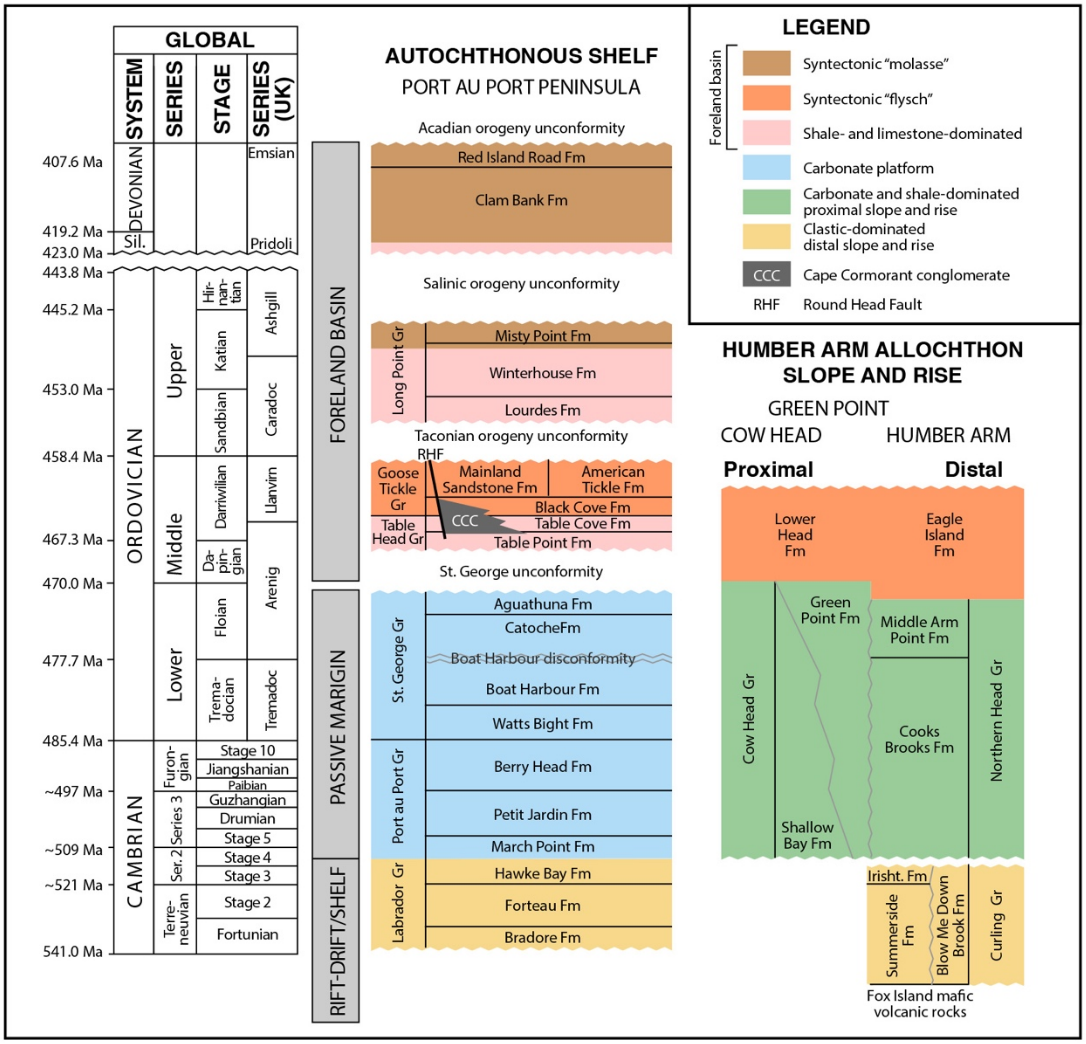

Fig. 2

Regional tectonostratigraphy and correlations of the authochthonous shelf sequences and the allochthonous Humber Arm allochthon. Modified after Cooper et al., 2001; Dietrich et al., 2011; Hinchey et al., 2015; Confliffe et al., 2017. Numbers in Million years (Ma) after Cohen, K.M., Finney, S.C., Gibbard, P.L., & Fan, J.-X. (2013; updated) The ICS Chronostratigraphic Chart. Episodes 36: 199-204. http://www.stratigraphy.org/ICSchart/ChronostratChart2017-02.pdf and the Ordovician Chronostratigraphic Chart of the International Subcommission on Ordovican Stratigraphy, 2017.

Fig. 3

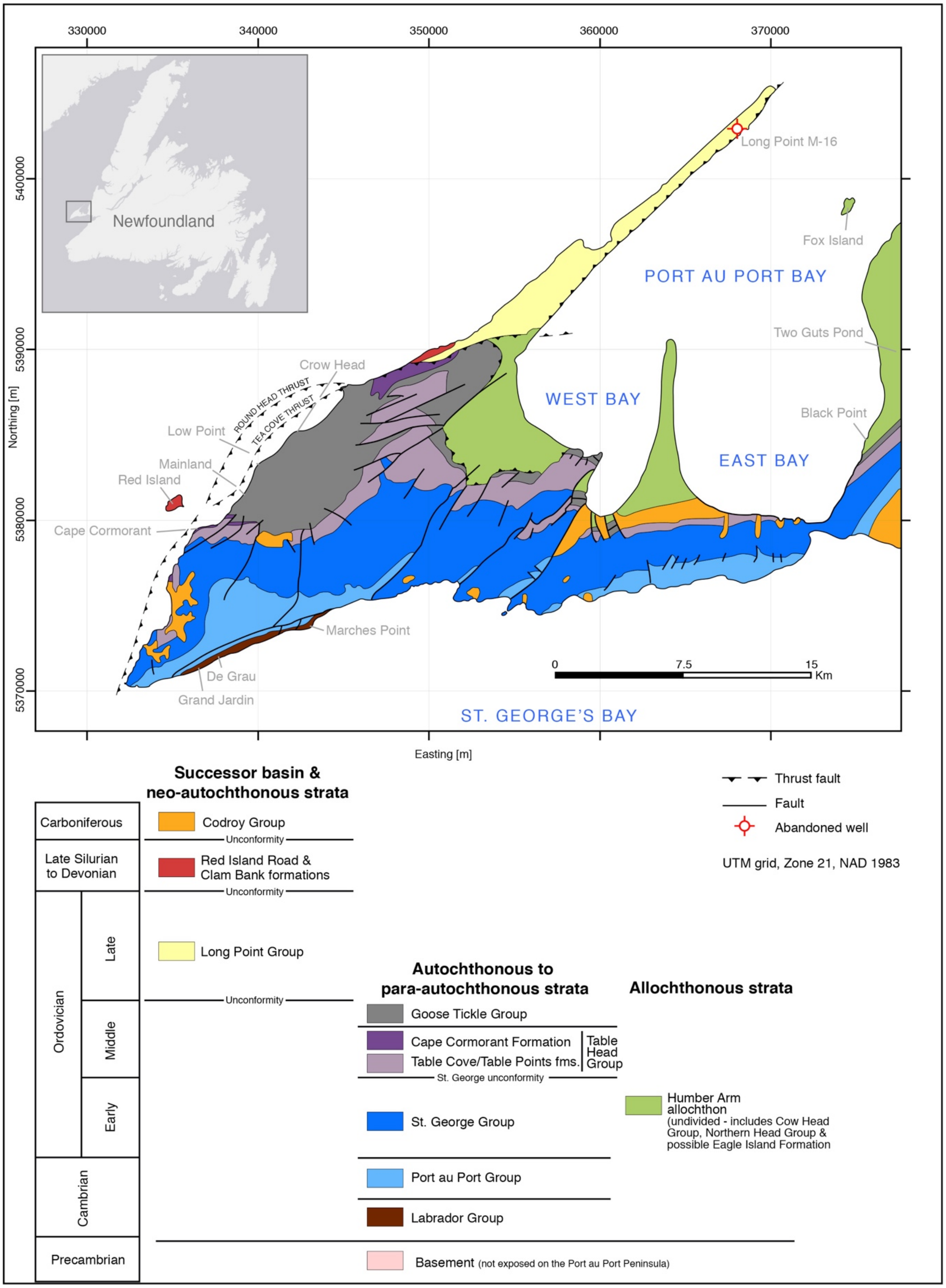

Fig. 3
Geological map of the Port au Port peninsula area. Modified from Hogg and Enachescu, 2015, and references therein.

Fig. 4

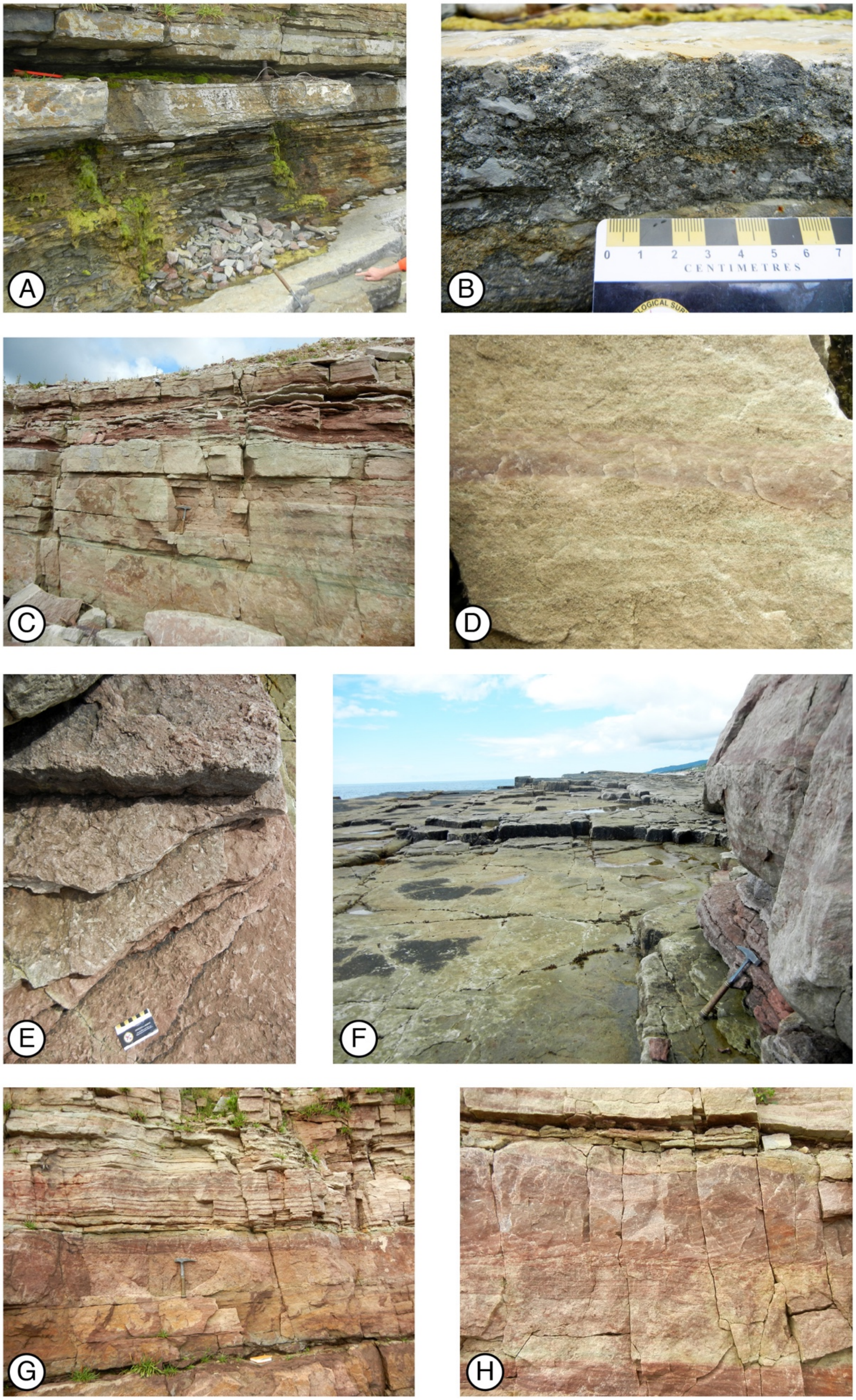

Fig. 4

Outcrop photographs of the Hawke Bay Formation, Port au Port peninsula.
A) Stratigraphic contact to the overlying Port au Port group marked by (B) a carbonate conglomerate layer. C) Coastal cliffs along the Marches Point area. D) Massive to thick-bedded grey-beige quartz arenite with intercalated silicified layer and vague cross-lamination. E-F) Bioturbated horizons. G-H) Coastal cliffs along the De Grau area, below the school.

Fig. 5

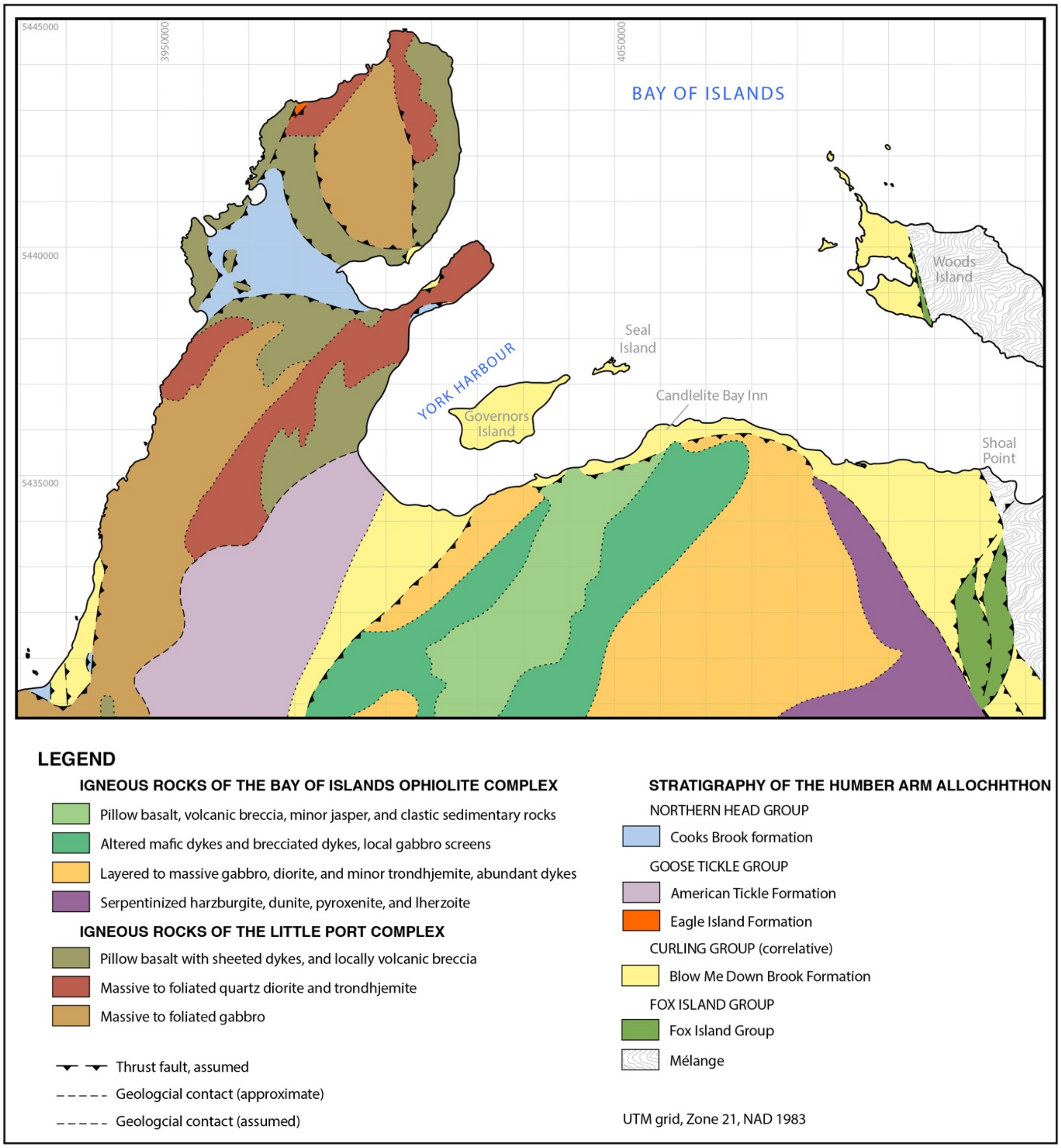

Fig. 5

Geological map of the Bay of Islands area, modified and simplified after Waldron et al., 2003 and Burden et al., 2006.

Fig. 6

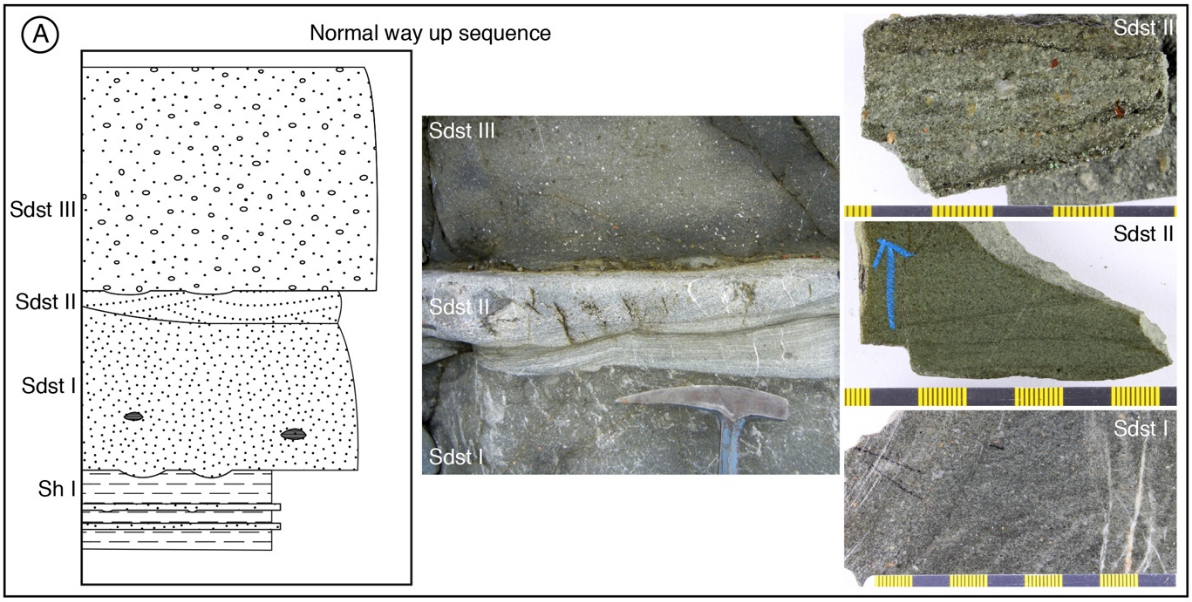
A
Normal way up sequence
Sdst III
Sdst II
Sdst I
Sh I
Sdst III
Sdst II
Sdst I
Sdst II
Sdst II
Sdst I

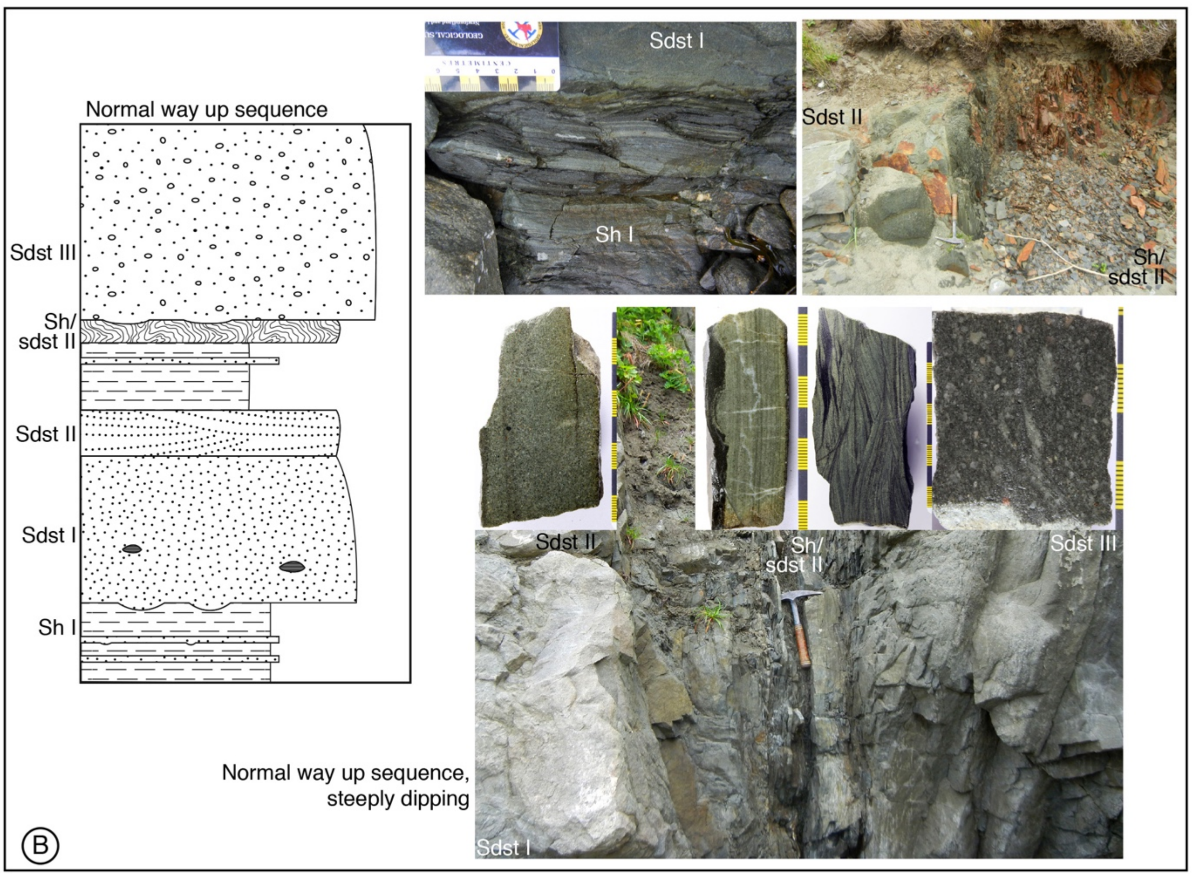
Normal way up sequence
Sdst III
Sh/
sdst II
Sdst II
Sdst I
Sh I
Sdst I
Sh I
Sdst II
Sh/
sdst II
Sdst II
Sh/
sdst II
Sdst III
Normal way up sequence,
steeply dipping
Sdst I
B

Fig. 6

A) Stratigraphic sequence (normal way up) of the Blow Me Down Brook Formation in the Candlelite Bay Inn area with the three main sandstone types (Sdst I: medium grey coarse-grained sandstone; Sdst II: light grey medium-grained sandstone; Sdst III: dark grey very coarse-grained to pebbly sandstone) and shales (Sh I) that are underlying the sandstones. Sketch of sequence in left-hand side of the figure, outcrop photo in the middle, and photographs of cut hand samples of the three sandstone types to the right. B) Normal way up stratigraphic sequence of the three main sandstone types (Sdst I, Sdst II, Sdst III) and a section of shales that are interbedded with sandstones (Sh/Sdst II). Upper photograph in the middle shows steeply dipping shales (Sh I) that are underlying the sandstones. Upper photograph to the right shows steeply dipping shales (Sh/Sdst II) that are overlying Sdst II. Lower photograph shows a steeply dipping sequence of Sdst I (on the ledge to the left), light grey bed of the medium-grained Sdst II that is overlain by a succession of shales interbedded with planar laminated medium-grained sandstone with scoured bases and a friable crosslaminated shaly sandstone layer (Sh/Sdst II) that is overlain by a thick bed of dark pebbly sandstone (Sdst III).

***Fig.** 7*

A) Normal way up stratigraphic sequence of the three main sandstone types (Sdst I, Sdst II, Sdst III) and a bed of cross-laminated Sh/Sdst II that overlies Sdst II and is overlain by Sdst III (middle upper photograph). Upper photograph to the right shows dark grey to black fissile shale chip that commonly occurs within Sdst I. Lower middle photograph shows a petroliferous fracture within Sdst III. Lower photograph to the right shows typical patchy calcite alteration characteristic for Sdst I. B) Overturned stratigraphic sequence of the three main sandstone types with red shales stratigraphically underlying Sdst I now on top of the succession (upper middle photograph). Upper photograph to the right shows a tight detached fold hinge with Sdst II and adjacent shales that may be related to thrusting and the emplacement of the ophiolotic mappes of the Blow Me Down Brook mountains. If thrust-related folding is present, it may explain the overturned beds. Folding could also be synsedimentary slump structure (Calon, 2017, pers. comm.).

Fig. 7

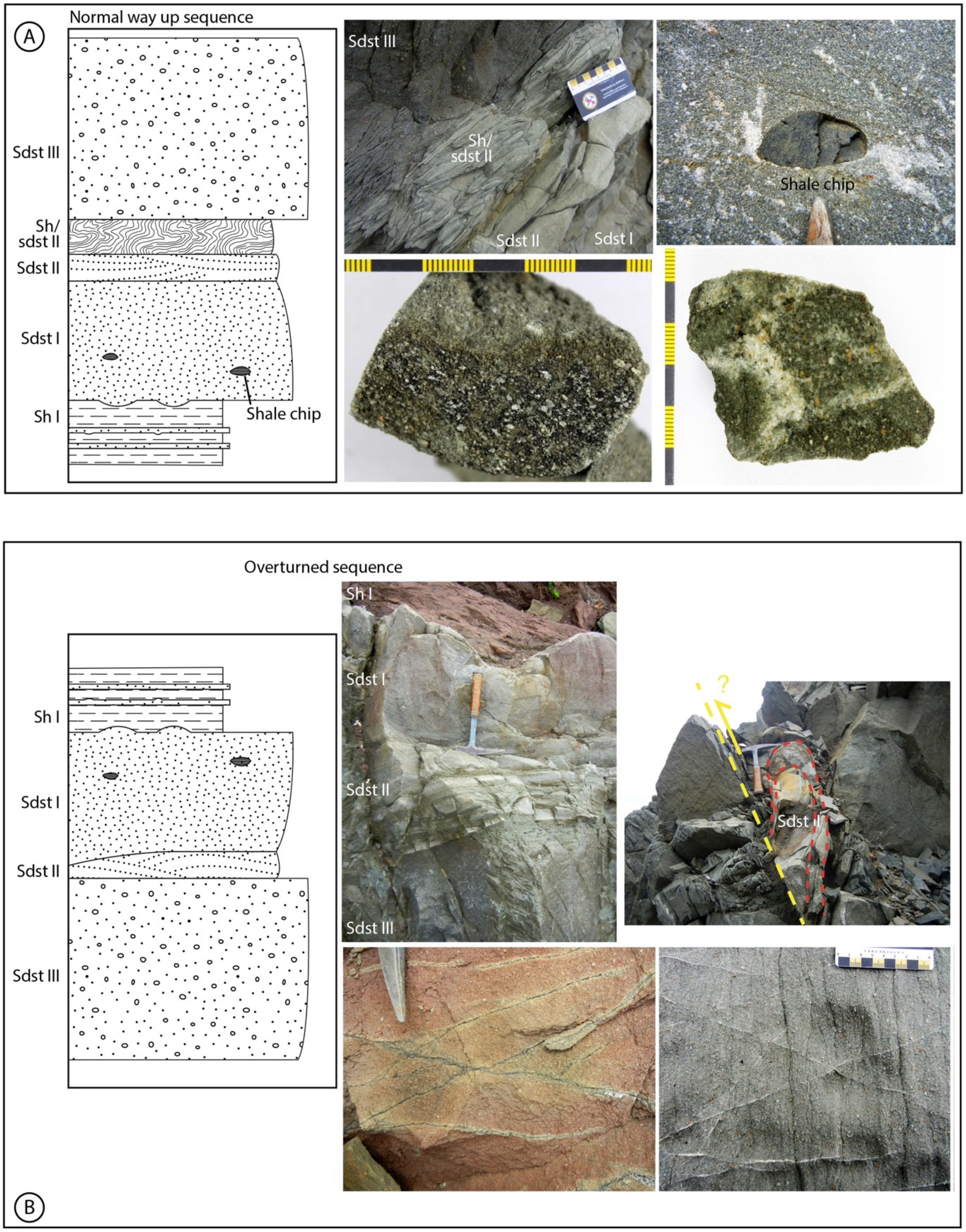
A
Normal way up sequence
Sdst III
Sh/
sdst II
Sdst II
Sdst I
Sh I
Shale chip
Sdst III
Sh/
sdst II
Sdst II
Sdst I
Shale chip
Overturned sequence
Sh I
Sdst I
Sdst II
Sdst III
?
Sdst II
B

Fig. 8

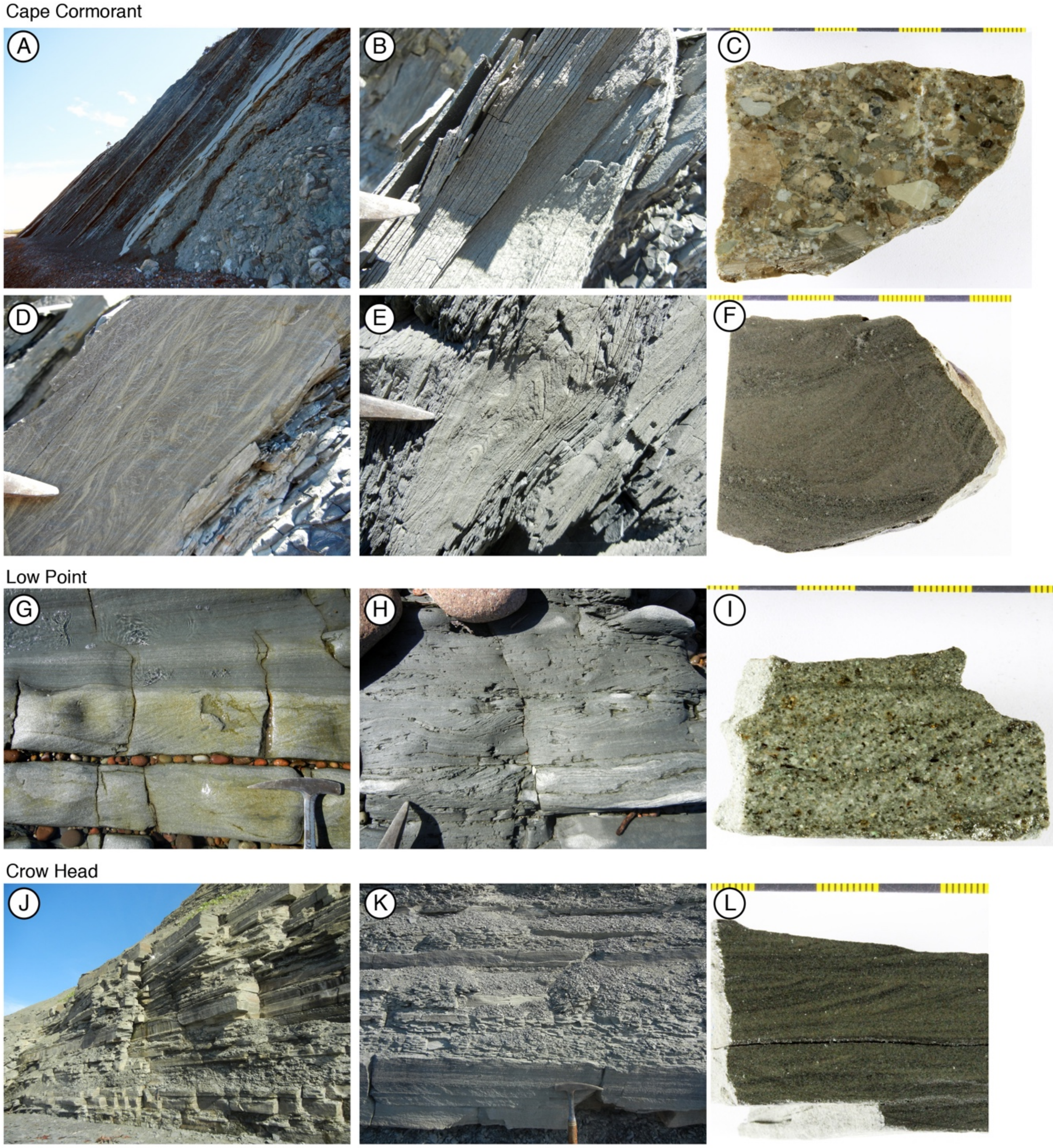

Fig. 8

Outcrop photographs of the Cape Cormorant to Mainland section and photographs of cut hand samples of the Mainland Sandstone Formation overlying the Cape Cormorant Formation conglomerates. A) Succession of shales interbedded with sandstones of the Mainland Sandstone Formation overlying the Cape Cormorant Formation conglomerates. B) Planar lamination within Mainland Sandstone Formation sandstones. C) Photograph of a cut rock sample of a carbonate conglomerate immediately underlying the thick bed of the boulder conglomerate of the Cape Cormorant Formation. D-F) Cross-lamination and slump structures within sandstones of the Mainland Sandstone Formation. G-H) Shoreline outcrop photographs of cross-laminated sandstones intercalated with shales of the Low Point area. I) Photograph of a cut rock samples of porous coarse-grained sandstone from the Low Point area of the Mainland Sandstone Formation. J-K) Outcrop photographs of the cliffs in the Crow Head area, Mainland Sandstone Formation. L) Photograph of a cut rock sample of a cross-laminated sandstone of the Crow Head Mainland Sandstone Formation.

Fig. 9

Eagle Island Formation / Middle Arm Point Formation

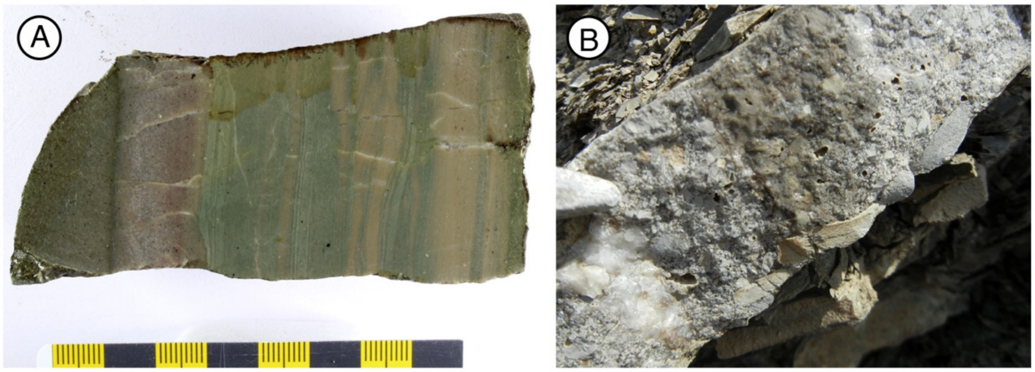

Lower Eagle Island Formation

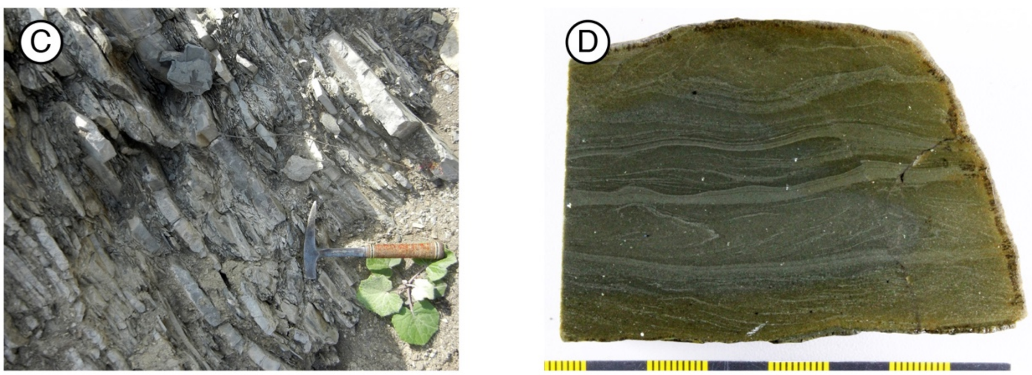

Eagle Island Formation / Black Point

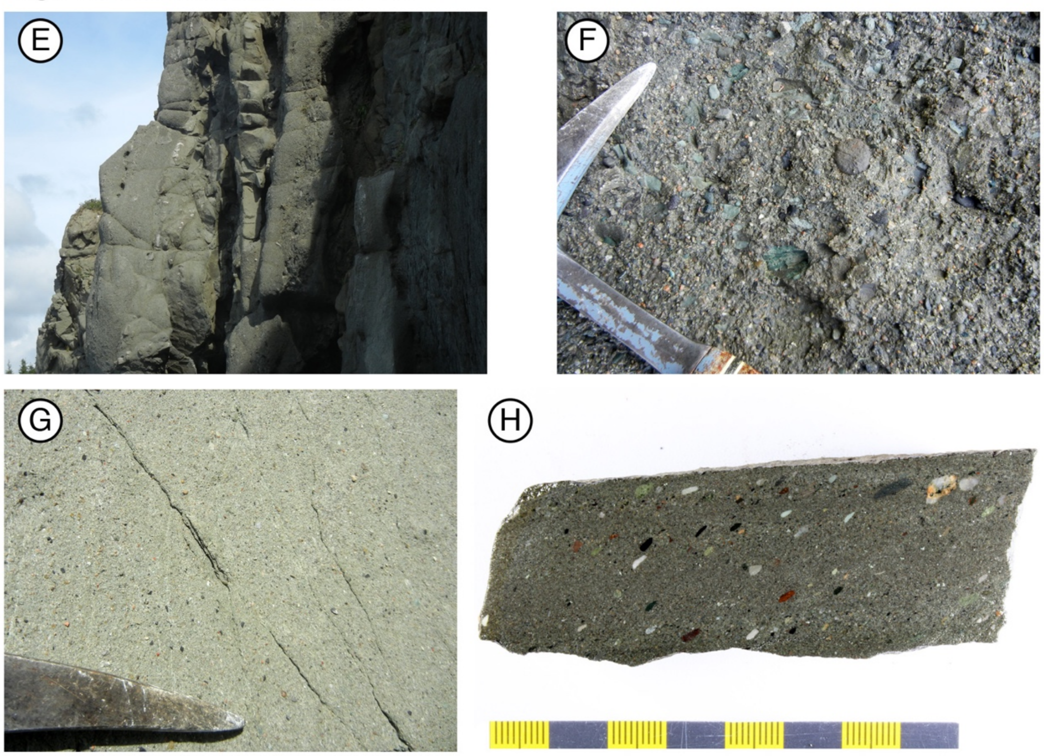

Fig. 9

A) Intercalated red and green silicified shales and siltstones of the uppermost Middle Arm Point Formation, north of Black Point cliffs. B) Carbonate conglomerate layer of the uppermost Middle Arm Point Formation, north of Black Point cliffs. C) Intercalated shales and sandtones of the lower Eagle Island Formation, north of Black Point cliffs. D) Sandstone from (C) with synsedimentary slump structures. E) Stepply dipping thick amalgated sandstone and conglomerate beds of the Eagle Island Formation at Black Point. F) Outcrop photograph of a conglomerate layer of the Eagle Island Formation at the Black Point cliffs. G) Outcrop photograph of a pebbly sandstone layer of the Eagle Island Formation at the Black Point cliffs. H) Photograph of a cut rock samples of the pebbly sandstone of (G) with a preferred orientation of the pebbly framework grains.

Fig. 10

Blow Me Down Formation or Eagle Island Formation at Two Guts Pond. A) Outcrop photograph of a petroleum-stained bed of a coarse-grained friable sandstone. B-D) Coarse-grained friable sandstone with cross-cutting (B-C) and bedding parallel (D) petroliferous fractures. E) Outcrop photograph of pebbly sandstones at Two Guts Pond. F) Outcrop photograph of conjugate set of joints cross-cutting Two Guts Pond sandstone. G) Pebbly sandstone of the Blow Me Down Brook Formation in the Candlelite Bay Inn area and H) Photograph from Quinn (1985) of pebbly sandstone of the Sellars (Blow Me Down Brook) Formation that are similar in appearance and type of weathering as the Two Guts Pond sandstones.

Fig. 11

Sample and outcrop locations of the Blow Me Down Brook Formation in the Bay of Islands area, Candlelite Bay Inn area (A-B), the Hawke Bay Formation, Marches Point and De Grau, and the Mainland Sandstone Formation, Cape Cormorant-Mainland, Low Point, Crow Head (B), Eagle Island Formation, Black Point (B), and the Two Guts Pond sandstones (B).

Fig. 10

Two Guts Pond

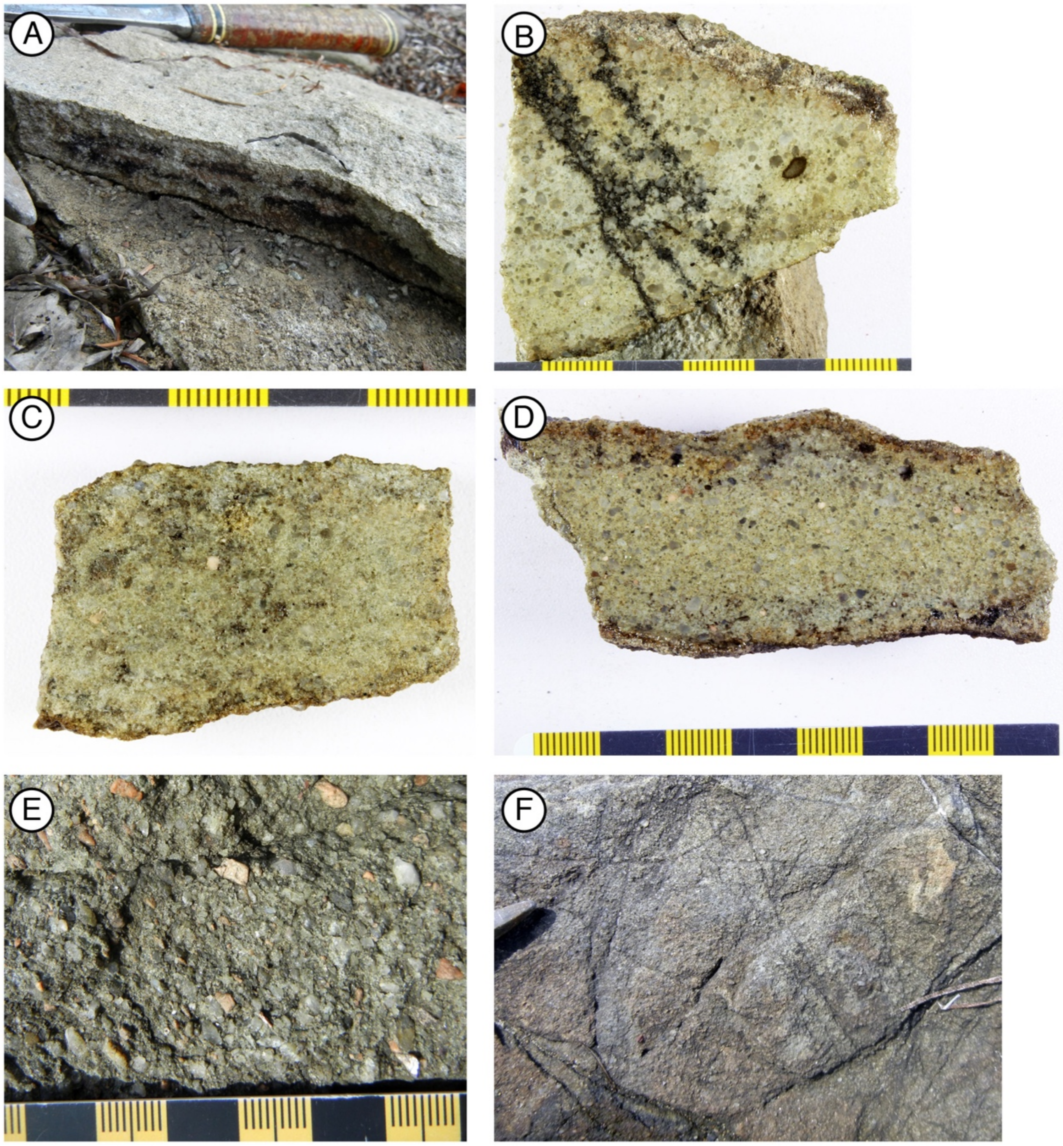

Blow Me Down Brook Formation
Candleite Bay Inn area

Blow Me Down Brook Formation/ Sellars Formation
(from Quinn, 1985)

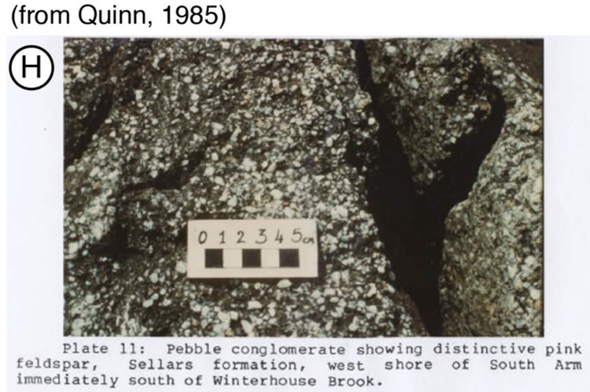

Fig. 11

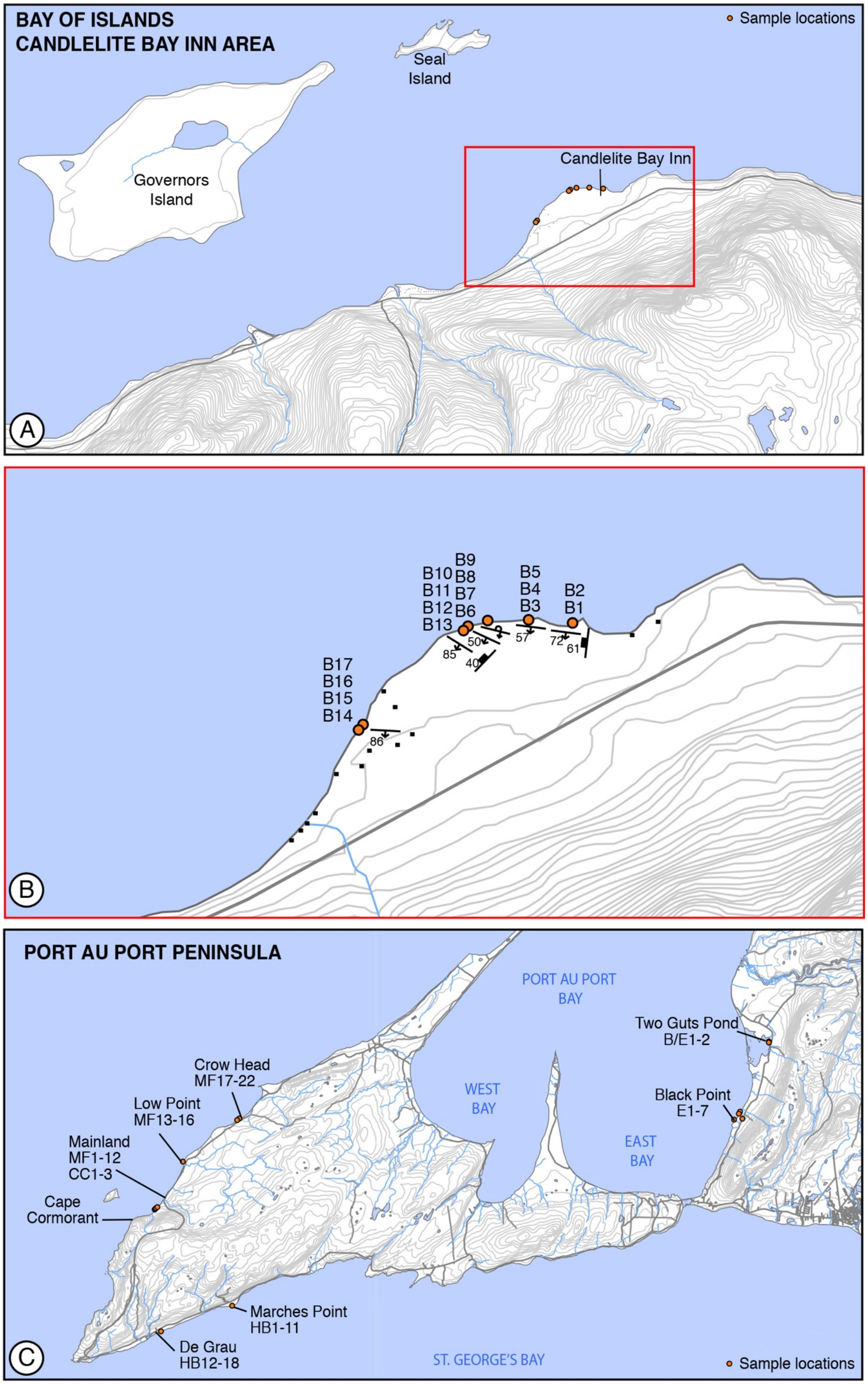
BAY OF ISLANDS
CANDLELITE BAY INN AREA
Sample locations
Seal Island
Governors Island
Candlelite Bay Inn
A
B10
B11
B12
B13
B9
B8
B7
B6
B5
B4
B3
B2
B1
B17
B16
B15
B14
85
50
40
57
72
61
86
B
PORT AU PORT PENINSULA
PORT AU PORT BAY
WEST BAY
EAST BAY
Two Guts Pond
B/E1-2
Black Point
E1-7
Crow Head
MF17-22
Low Point
MF13-16
Mainland
MF1-12
CC1-3
Cape Cormorant
Marches Point
HB1-11
De Grau
HB12-18
ST. GEORGE'S BAY
Sample locations
C

Fig. 12

SEM-MLA MAPS
COLOUR CODE

Quartz
Plagioclase
Albite
K-spar
Calcite
Siderite
Ankerite
Dolomite
Apatite
Apatite -phosph. shale
Barite
Muscovite
Biotite
Chlorit-Fe
Kaolinite
Illite
Glauconite
Clinochlore
Garnet
Pyrite
Sphalerite
Chalcopyrite
Fe-oxide (hematite or magnetite)
Chromite
Titanite
Olivine
Xenotime-(Y)
Ilmenite
Ilmenorutile
Rutile
Rutile-Ilm mix
Monazite-(Ce)
Zircon
Thorite
Organic
Pores
Calc-qtz-mix (in CC and MF samples)

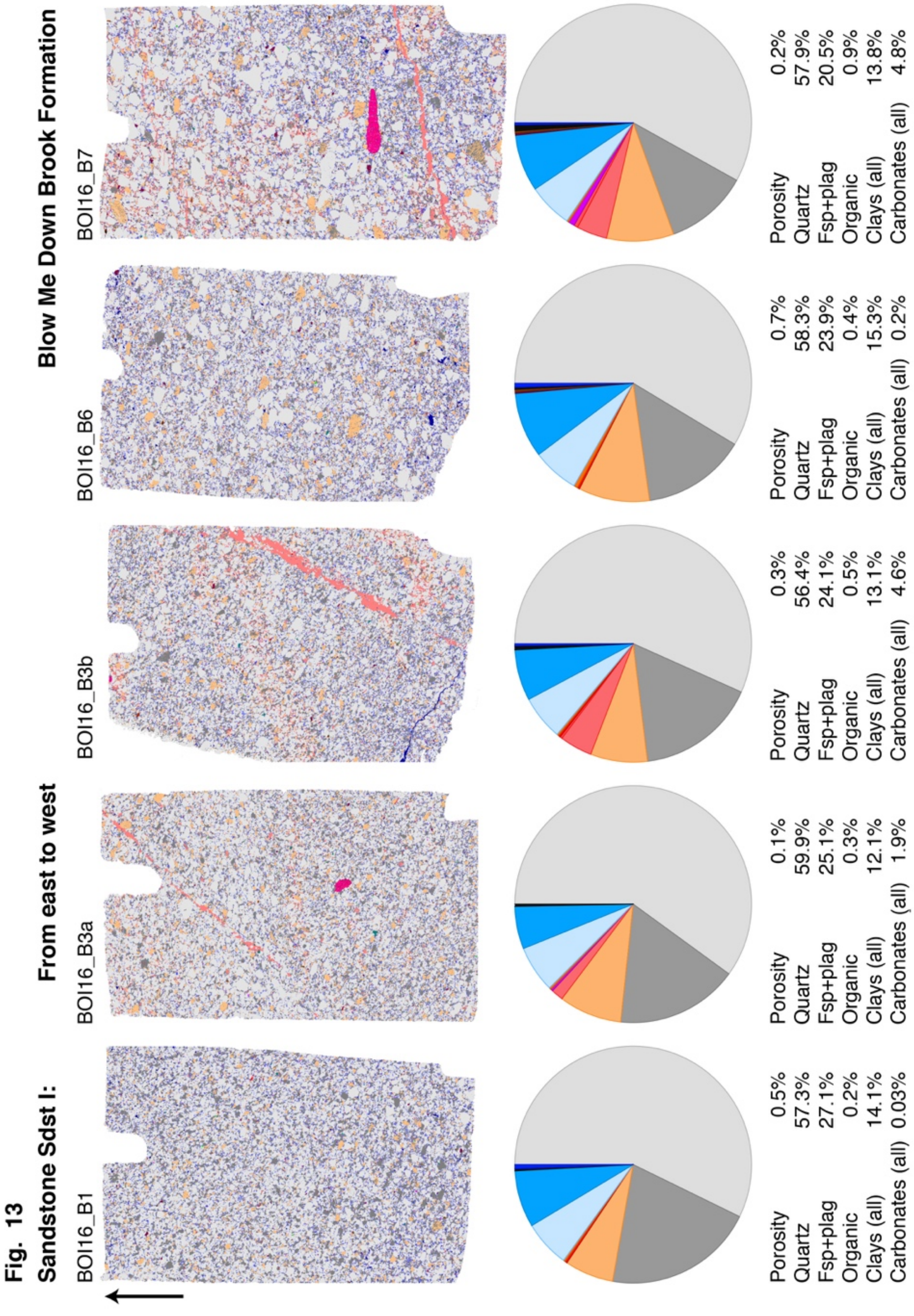

Fig. 13

SEM-MLA maps and pie charts of the basal sandstones (Sdst I) of the Blow Me Down Brook Formation.

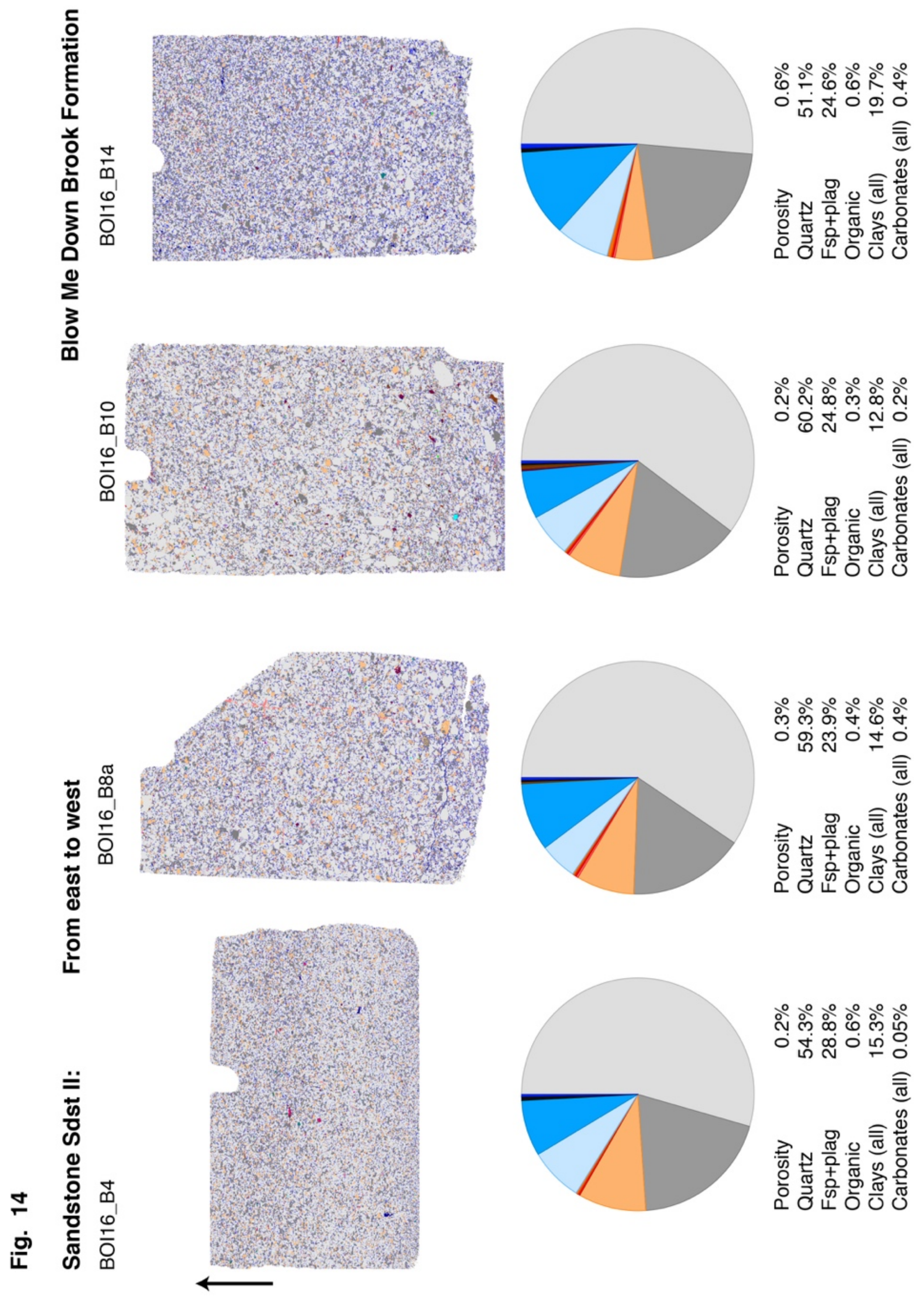

Fig. 14

SEM-MLA maps and pie charts of the light grey weathering sandstones (Sdst II) of the Blow Me Down Brook Formation.

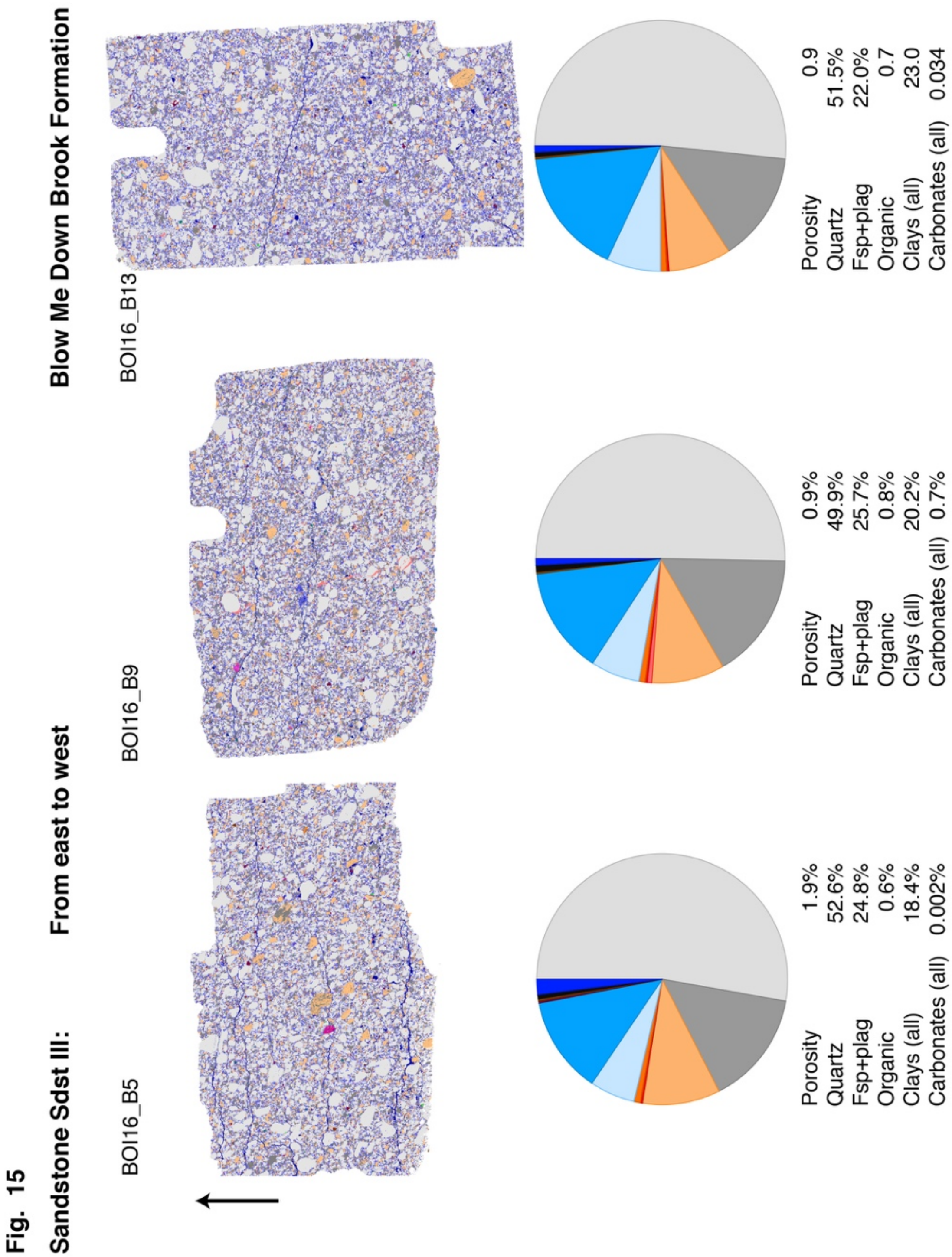

Fig. 15

SEM-MLA maps and pie charts of the upper sandstones (Sdst III) of the Blow Me Down Brook Formation.

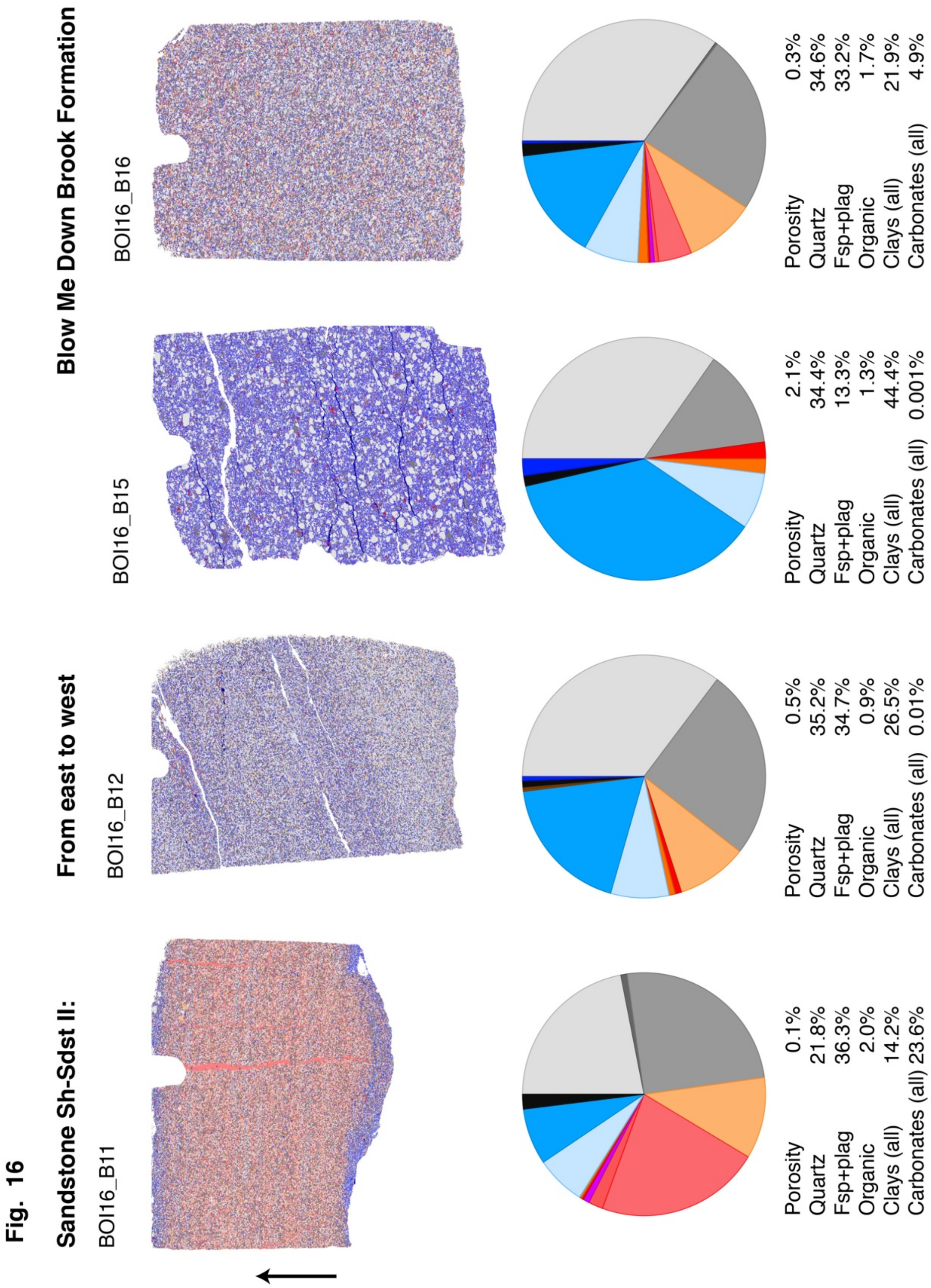

Fig. 16

SEM-MLA maps and pie charts of the sandstones that are intercalated with shales (Sh/Sdst II) of the Blow Me Down Brook Formation.

Fig. 17

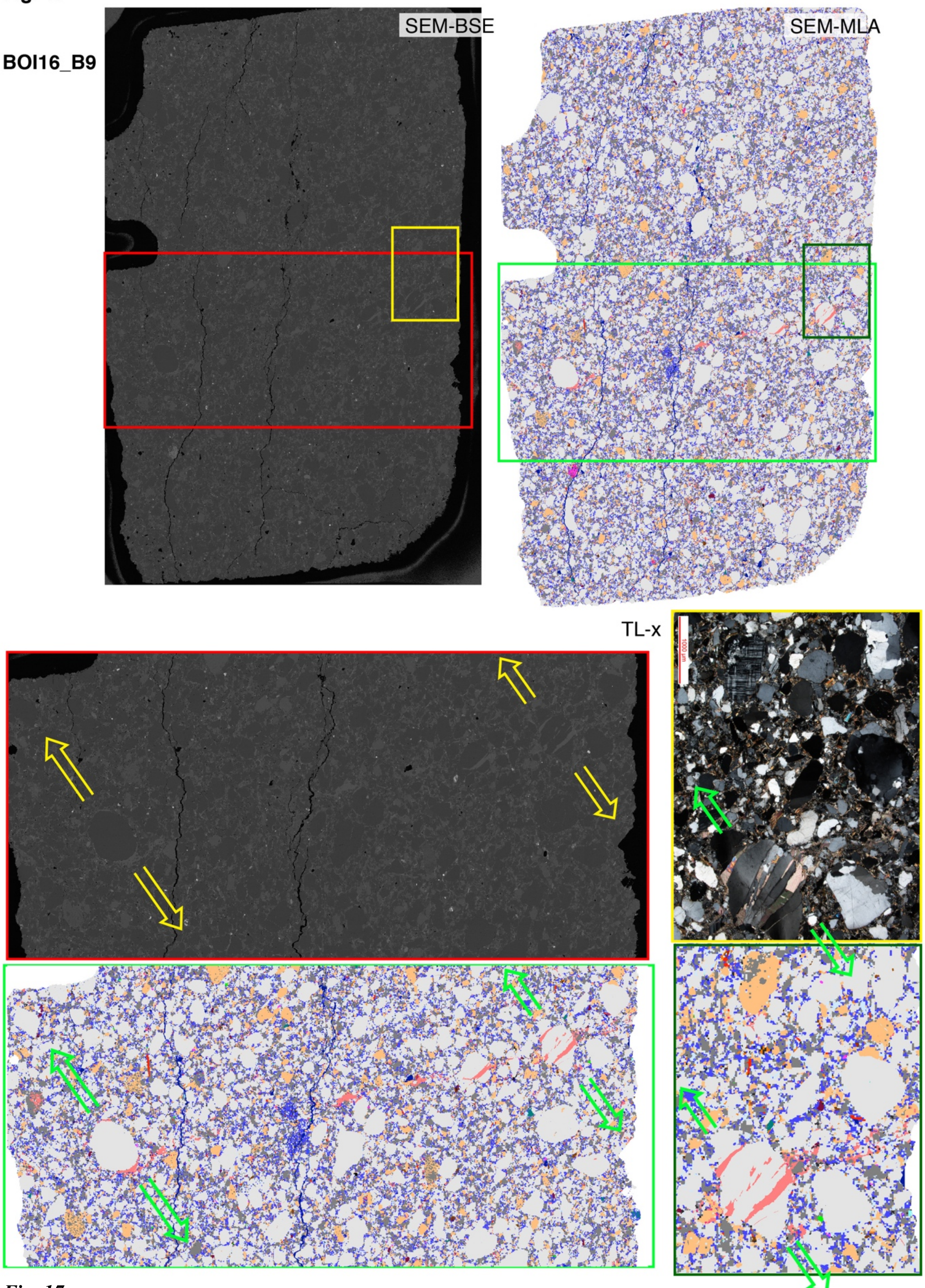

Fig. 17

SEM-BSE and related SEM-MLA map of an upper sandstone (Sdst III) sample (BOI16_B9) and close-ups of these maps with related transmitted light (crossed nicols, TL-x) micrographs showing calcite filling extensional veins and forming pressure shadow mineralization rims around a quartz grain (lower left pink calcite in pressure shadows around a rounded grey quartz grain.

Fig. 18

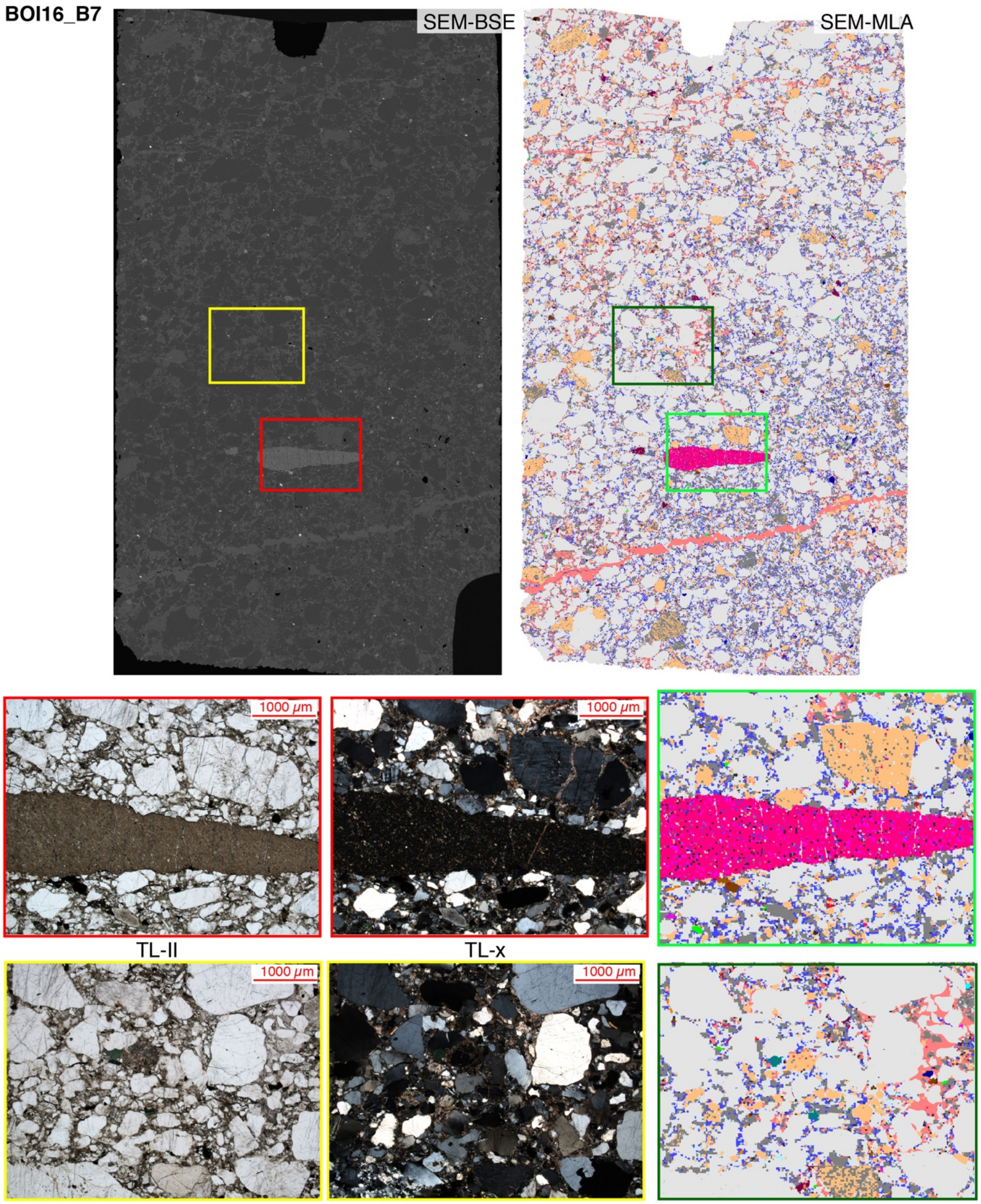

Fig. 18

SEM-BSE and related SEM-MLA map of an upper sandstone (Sdst I) sample (BOI16_B7) and close-ups of these maps with related transmitted light (crossed nicols, TL-x, and parallel nicols, TL-II) micrographs showing phosphatized shale chip (pink phleb), K-feldspars (orange) with albite (medium-dark grey) alteration.

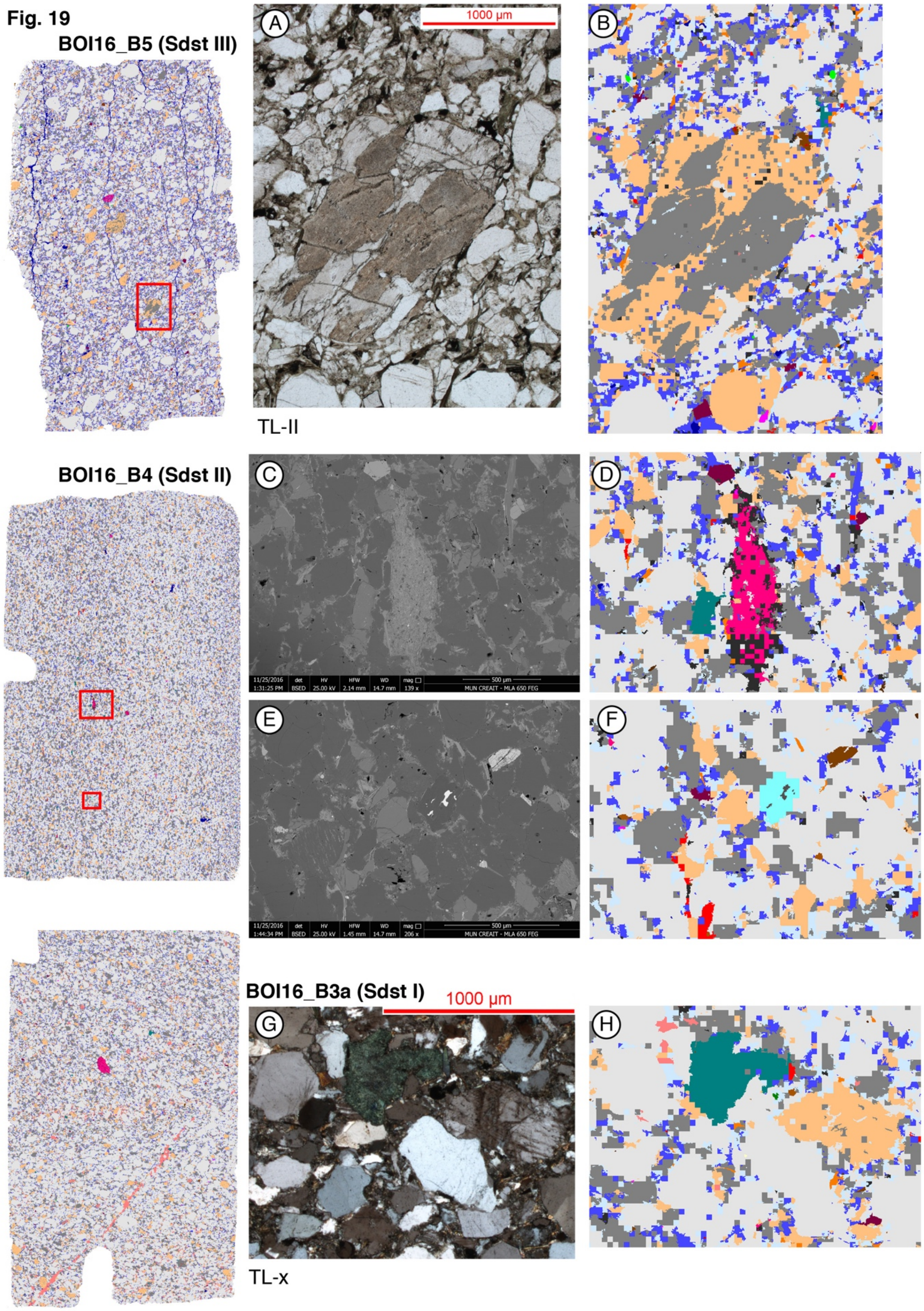

Fig. 19

SEM-BSE and related SEM-MLA map of an upper sandstone (Sdst III) sample (BOI16_B5) and sandstone (Sdst II) sample (BOI16_B4) and close-ups of these maps with related transmitted light (crossed nicols, TL-x, and parallel nicols, TL-II) micrographs. A-B) Albite (medium-dark grey)-altered K-feldspar (orange). C-D) Phosphatized shale chip (pink) and glauconite (blue-green) phleb and garnet fragment (burgundy). E-F) Chromite (dark grey) within clinochlore (bright light blue), rutile (brown), and detrital muscovite (red). G-H) Glauconite (blue-green) phleb.

Fig. 20

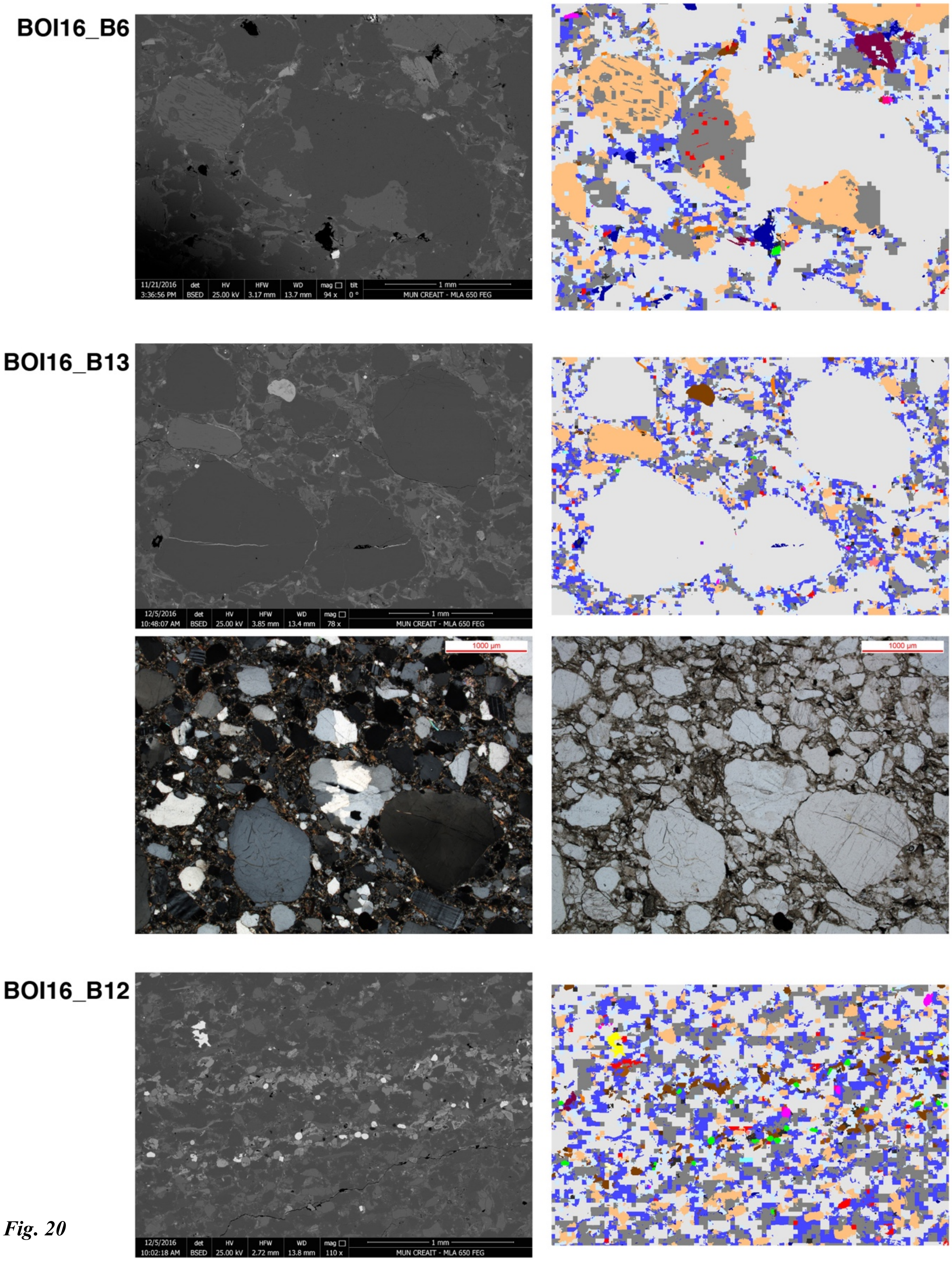

Fig. 20

SEM-BSE and related SEM-MLA close-ups. BOI16_B6: of an igneous lithic fragment with quartz in association with seritized albite (medium-dark grey with red specs) and K-feldspar. BOI16_B13: Partially porous and partially barite-filled crack in quartz. BOI16_B12: Bands of heavy minerals (rutile, ilmenite, garnet, chromite, zircon, monazite, chalcopyrite, and apatite) in a medium-grained shaley sandstone (Sh/sdst II).

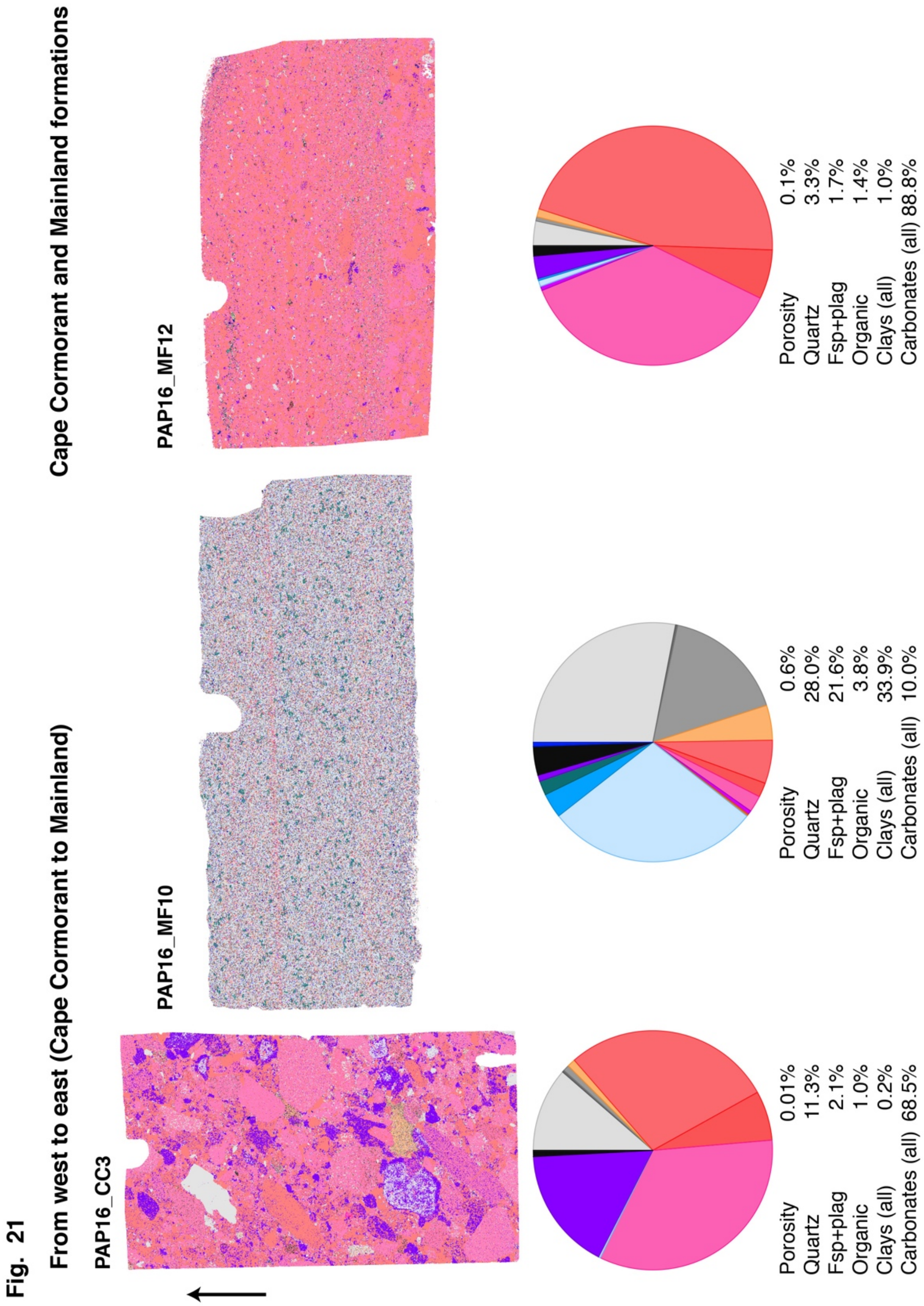

Fig. 21

SEM-MLA maps and pie charts of the Cape Cormorant Formation conglomerate and overlying sandstone and calcarenite of the Mainland Sandstone Formation from the Cape Cormorant and Mainland area.

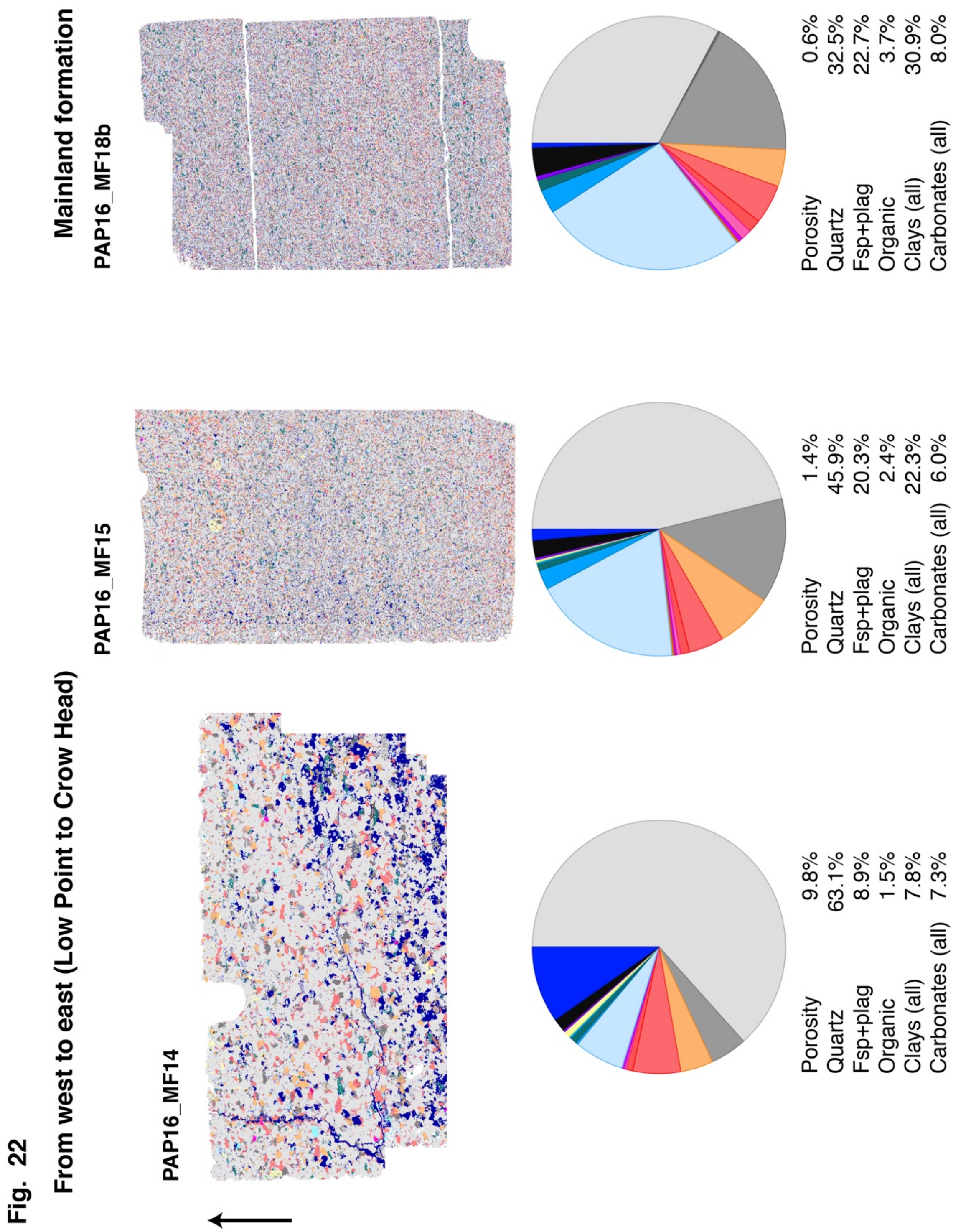

Fig. 22

SEM-MLA maps and pie charts of the sandstone of the Mainland Sandstone Formation from the Low Point and Crow Head areas.

Fig. 23

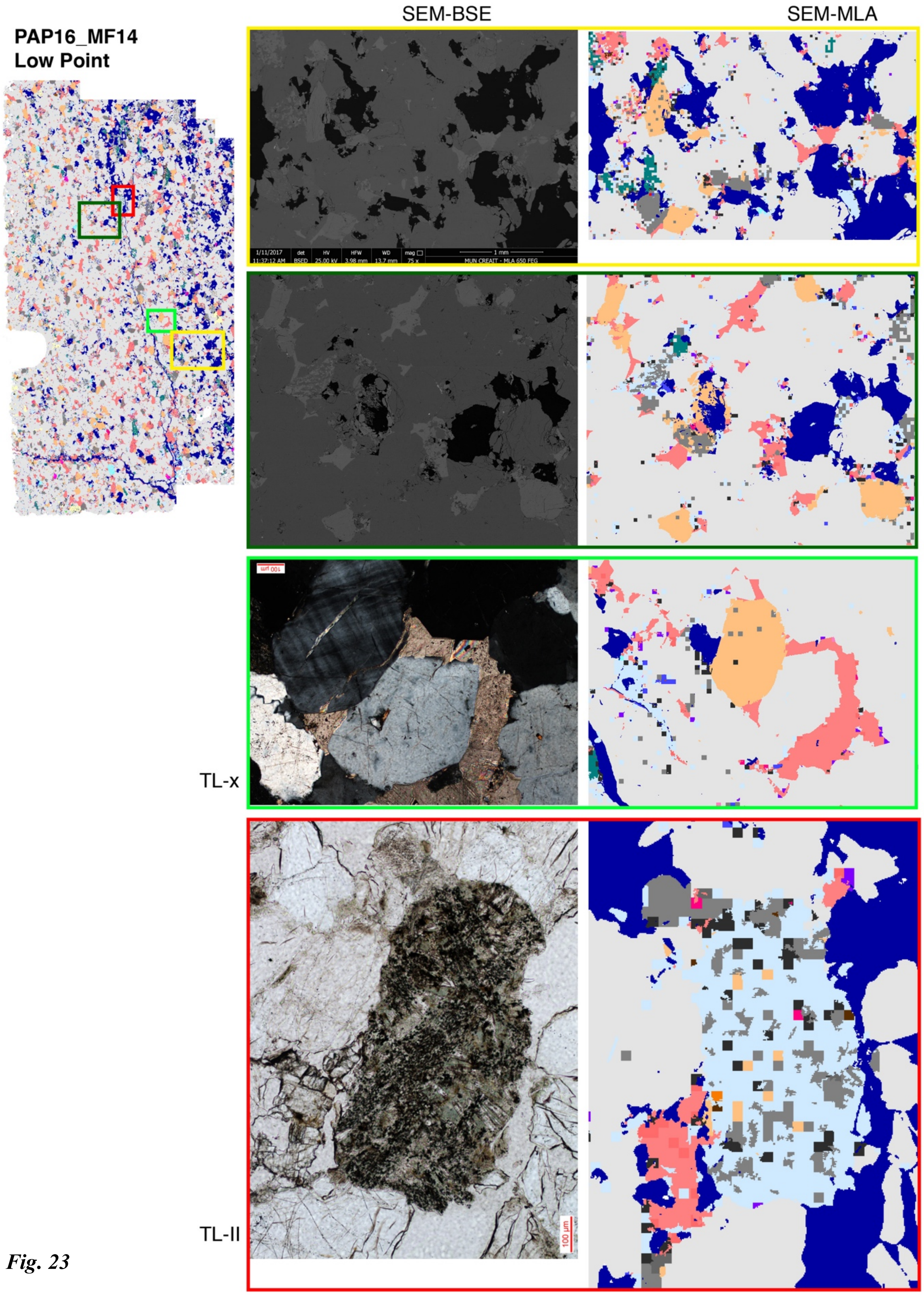

Fig. 23

SEM-BSE and related SEM-MLA map and close-ups of an porous sandstone sample (PAP16_MF14) of the Low Point area and related transmitted light (crossed nicols, TL-x, and parallel nicols, TL-II) micrographs. Porosity is not affected by compaction and secondary in nature due to dissolution of K-feldspar (upper four close-ups). Middle close-ups show microcline feldspar and quartz with calcite cement and related porosity. Lower to close-ups show a chloritized serpentinite grain and porosity (epoxy in the TL-II micrograph).

Fig. 24

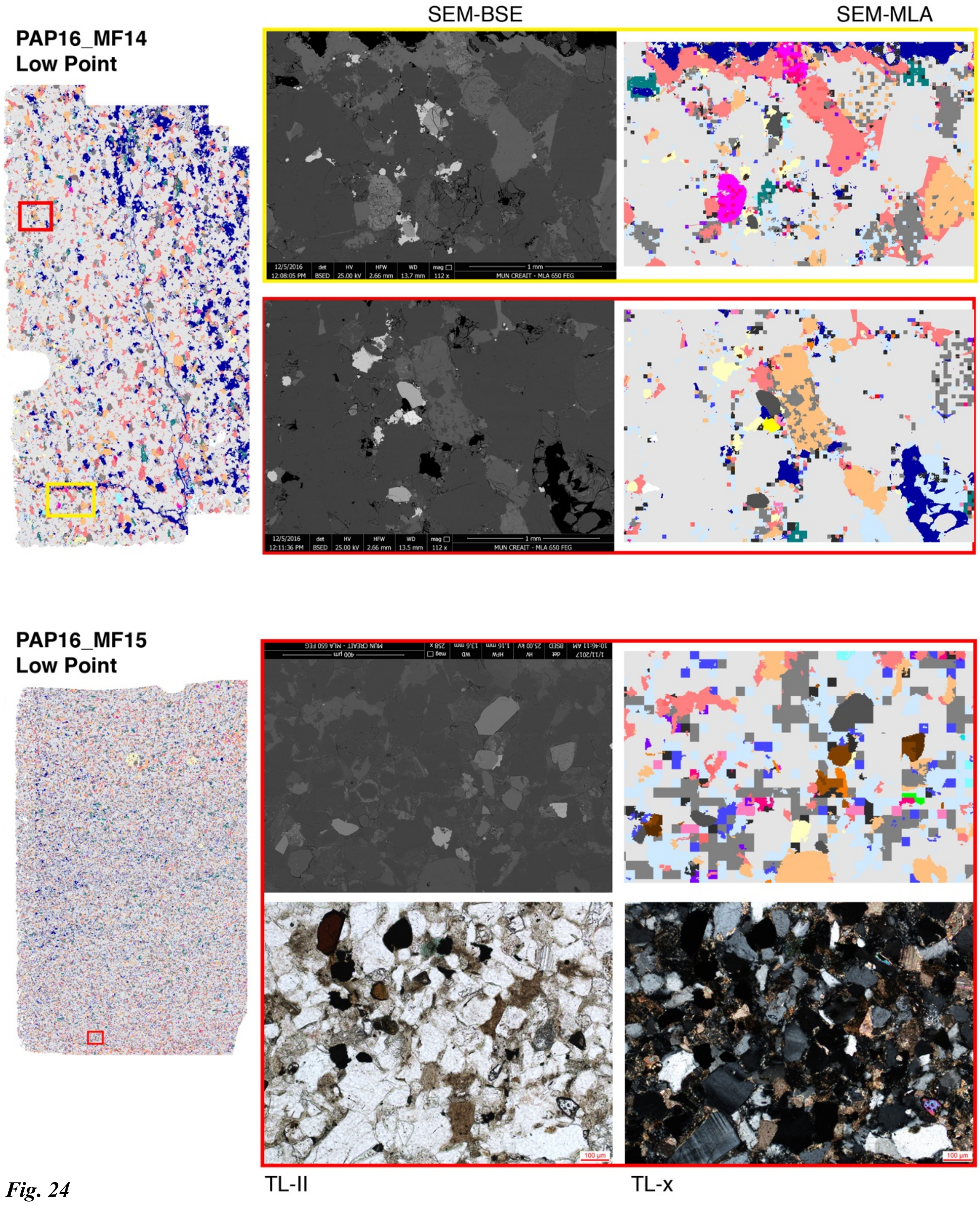

Fig. 24

SEM-BSE and related SEM-MLA map and close-ups of an porous sandstone sample (PAP16_MF14) of the Low Point area showing fracture porosity, calcite cementation, and chromite (dark grey) adjacent to an albite (medium-dark grey)-altered K-feldspar (orange). PAP16_MF15 is a medium-grained sandstone containing chromite (dark grey), rutile, ilmenite, and ilmenorutile (various shades of brown). Note, TL-II and TL-x micrographs need to be rotated ~30 degree to show the same orientation as in the SEM-BSE and SEM-MLA close-ups above.

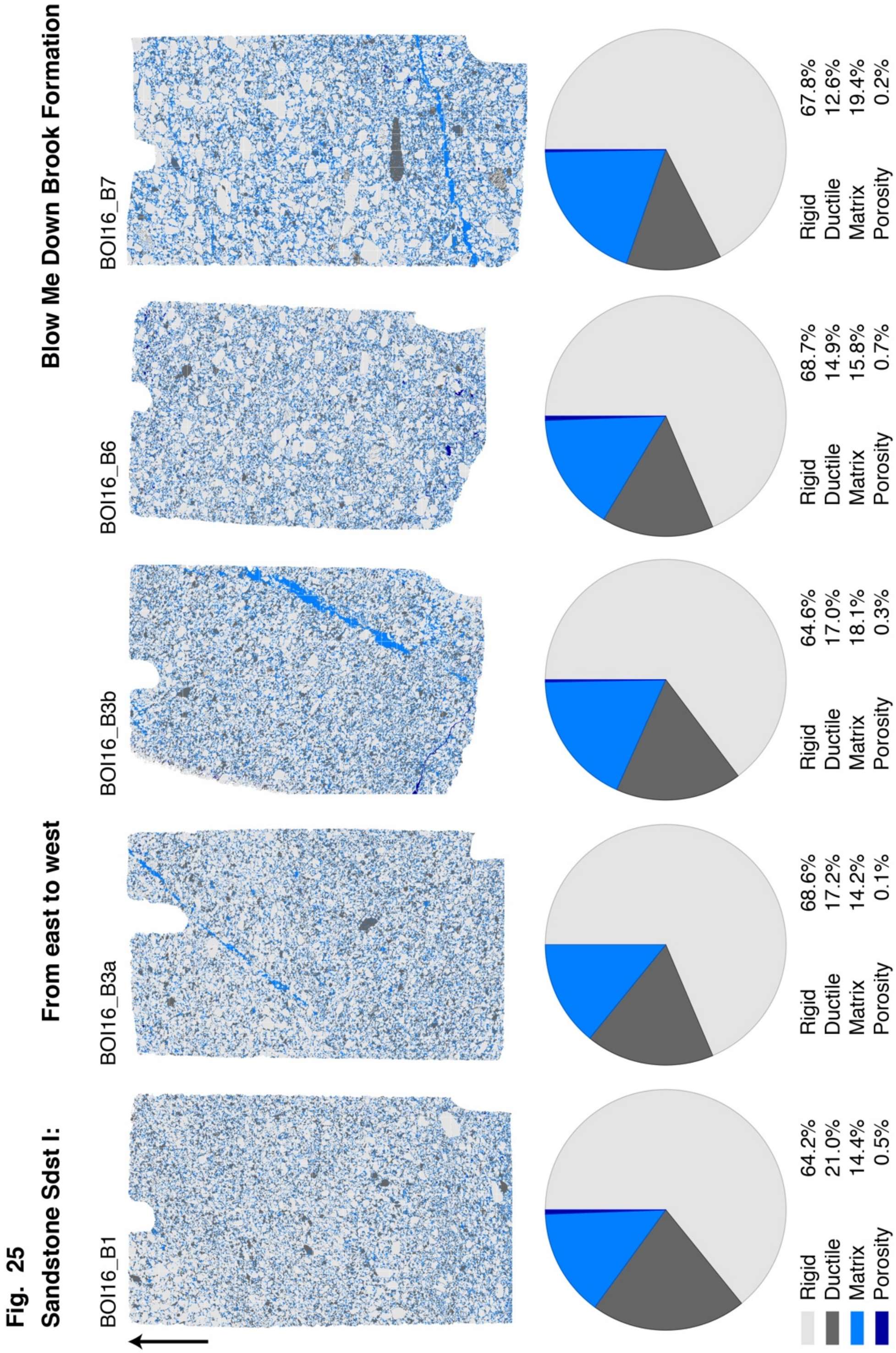

Fig. 25

SEM-MLA maps and pie charts of the grouped basal sandstones (Sdst I) of the Blow Me Down Brook Formation.

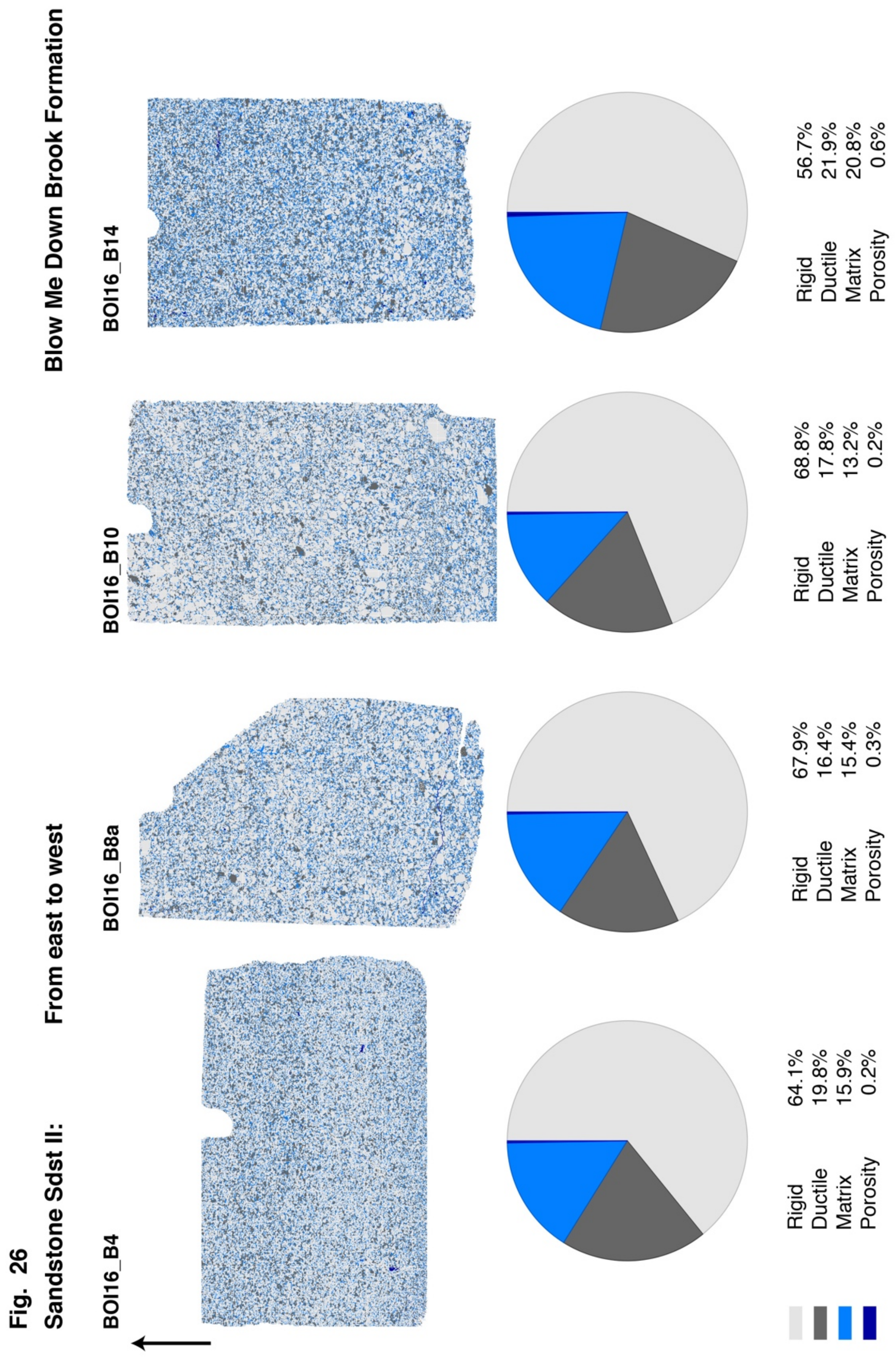

Fig. 26

SEM-MLA maps and pie charts of the grouped light grey weathering sandstones (Sdst II) of the Blow Me Down Brook Formation.

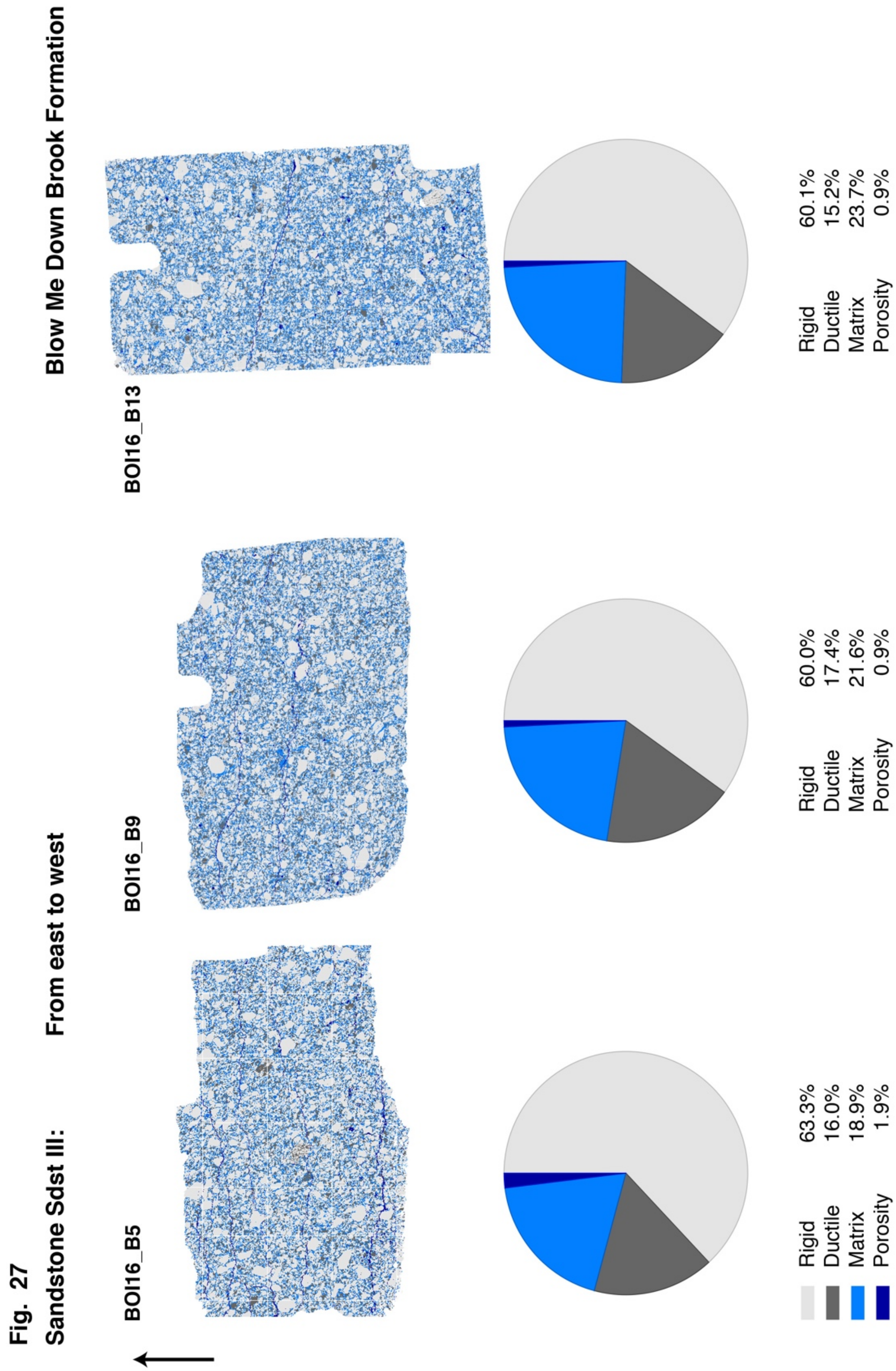

Fig. 27

SEM-MLA maps and pie charts of the grouped upper sandstones (Sdst III) of the Blow Me Down Brook Formation.

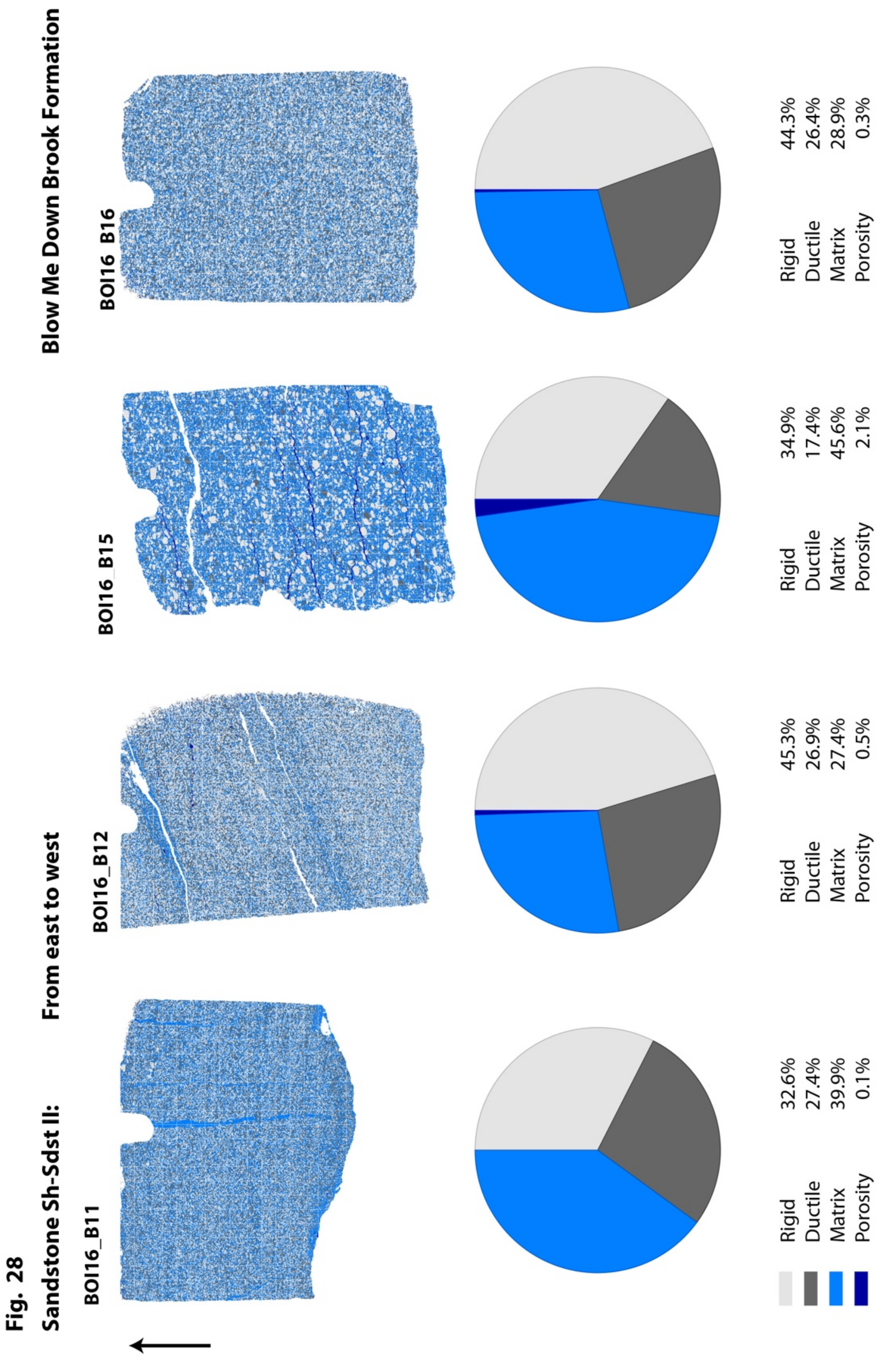

Fig. 28

SEM-MLA maps and pie charts of the grouped sandstones that are intercalated with shales (Sh/Sdst II) of the Blow Me Down Brook Formation.

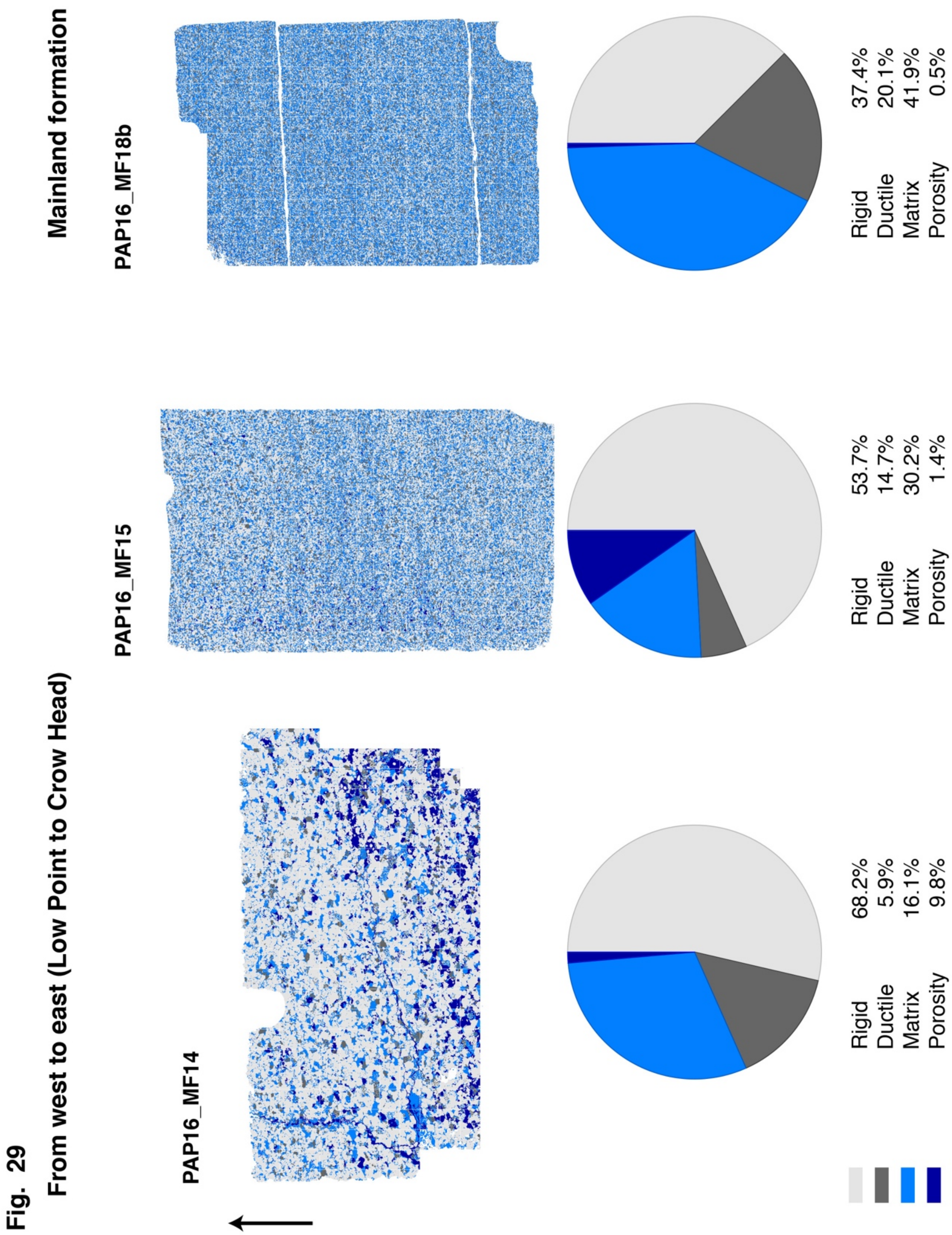

Fig. 29

SEM-MLA maps and pie charts of the grouped Cape Cormorant Formation conglomerate and overlying sandstone and calcarenite of the Mainland Sandstone Formation from the Cape Cormorant and Mainland area.

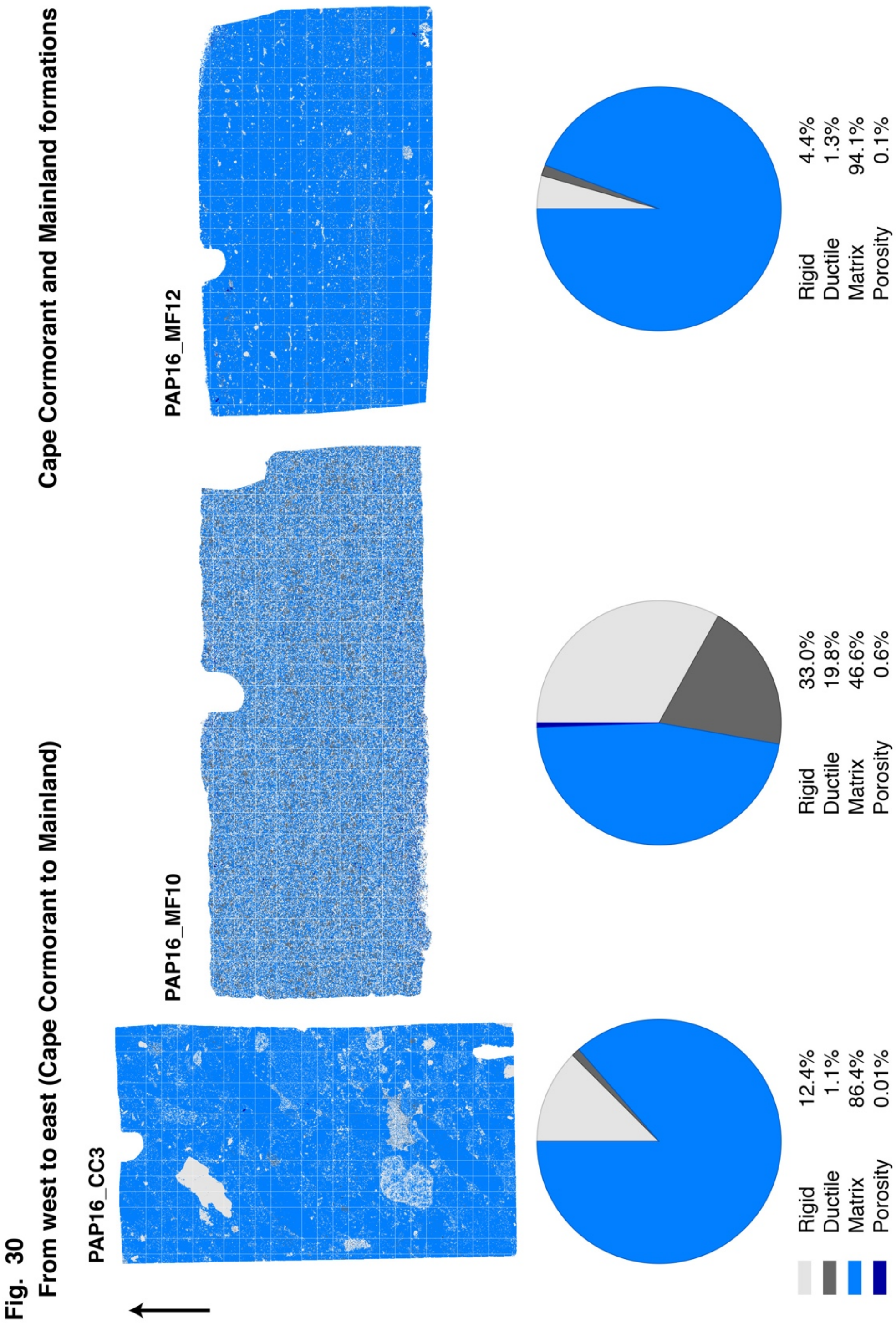

Fig. 30

SEM-MLA maps and pie charts of the grouped sandstone of the Mainland Sandstone Formation from the Low Point and Crow Head areas.

SEM-MLA data of samples in Area% of thin-section (ungrouped)

Mineral	BOI16_B1	BOI16_B2	BOI16_B3a	BOI16_B3b	BOI16_B4
Quartz	57.24875	51.61942	59.58879	56.39236	54.26163
Plagioclase	0.00880	0.00593	0.04198	0.05944	0.00522
Albite	20.44395	14.47916	16.53965	16.40132	19.28702
K-spar	6.64169	7.09254	8.54791	7.68474	9.51304
Calcite	0.02452	0.00834	1.79071	4.43524	0.04564
Siderite	0.00000	0.00000	0.00007	0.00014	0.00003
Ankerite	0.00320	0.00048	0.08400	0.13984	0.00058
Dolomite	0.00000	0.00006	0.00000	0.00000	0.00000
Apatite	0.03971	0.02163	0.04282	0.04183	0.03353
Phosph. Shale	0.01230	0.01741	0.19173	0.09976	0.06496
Barite	0.00021	0.00153	0.00061	0.01209	0.00320
Muscovite	0.20431	0.26855	0.12463	0.14412	0.14141
Biotite	0.16873	0.39944	0.17297	0.22944	0.19613
Chlorit-Fe	6.35416	6.94228	6.28135	6.16429	7.47450
Kaolinite	0.00124	0.00268	0.00156	0.00338	0.00293
Illite	7.76247	14.13104	5.72055	6.87495	7.76228
Glauconite	0.02327	0.04034	0.05267	0.04271	0.07207
Clinochlore	0.00598	0.01284	0.00701	0.00352	0.01053
Garnet	0.09885	0.06985	0.09388	0.10524	0.10810
Pyrite	0.00613	0.00724	0.00435	0.00775	0.00465
Sphalerite	0.00000	0.00000	0.00000	0.00000	0.00000
Chalcopyrite	0.00097	0.00116	0.00106	0.00175	0.00050
Fe-oxide	0.00183	0.00569	0.02764	0.03579	0.00167
Chromite	0.00032	0.00327	0.00181	0.00185	0.00077
Titanite	0.00225	0.00043	0.00128	0.00157	0.00012
Epidote	0.00000	0.00000	0.00000	0.00000	0.00000
Zoisite	0.00000	0.00000	0.00000	0.00000	0.00000
Olivine	0.00000	0.00000	0.00000	0.00000	0.00000
Xenotime-(Y)	0.00011	0.00007	0.00002	0.00050	0.00018
Ilmenite	0.00796	0.00887	0.05482	0.07682	0.01046
Ilmenorutile	0.03797	0.05954	0.03529	0.03340	0.02905
Rutile	0.06858	0.07151	0.08139	0.06724	0.05971
Rutile-Ilm mix	0.09468	0.13468	0.12152	0.11762	0.09580
Monazite-(Ce)	0.00339	0.00301	0.00253	0.00478	0.00361
Zircon	0.02676	0.02432	0.03440	0.02693	0.01762
Thorite	0.00000	0.00000	0.00001	0.00001	0.00000
Calc-qtz-mix	0.00000	0.00000	0.00000	0.00000	0.00000
Organic	0.23535	1.93562	0.28929	0.47496	0.60086
Clay	0.00000	0.03943	0.00000	0.00000	0.00000
Pores	0.46855	2.59158	0.05998	0.31101	0.19221
Unknown	0.00301	0.00000	0.00173	0.00361	0.00000
Low_Counts	0.00000	0.00000	0.00000	0.00000	0.00000
No_XRay	0.00002	0.00007	0.00000	0.00004	0.00002
Total	100.00000	100.00000	100.00000	100.00000	100.00000

SEM-MLA data of samples in Area% of thin-section (ungrouped)

Mineral	BOI16_B5	BOI16_B6	BOI16_B7	BOI16_B8	BOI16-B8b
Quartz	52.55440	58.32449	57.91694	59.29235	60.86755
Plagioclase	0.00554	0.01063	0.10491	0.01088	0.01900
Albite	14.71366	14.12203	11.28146	15.77739	14.44088
K-spar	10.09299	9.80054	9.15972	8.13483	7.99988
Calcite	0.00179	0.13394	4.29221	0.39058	0.93898
Siderite	0.00000	0.00000	0.00002	0.00001	0.00000
Ankerite	0.00012	0.01630	0.48053	0.01715	0.04701
Dolomite	0.00000	0.00000	0.00000	0.00000	0.00000
Apatite	0.06091	0.03921	0.10570	0.05075	0.04721
Phosph. Shale	0.07132	0.02700	0.73072	0.03205	0.11121
Barite	0.00283	0.00145	0.00066	0.00791	0.00256
Muscovite	0.20902	0.16411	0.08782	0.17723	0.16339
Biotite	0.86983	0.48007	0.28410	0.27550	0.39058
Chlorit-Fe	5.85160	6.44507	6.00620	5.21449	5.62427
Kaolinite	0.00059	0.00160	0.00114	0.00106	0.00197
Illite	12.46224	8.76658	7.70977	9.35247	7.98649
Glauconite	0.04386	0.04414	0.04048	0.04155	0.00984
Clinochlore	0.01180	0.01223	0.00803	0.00698	0.00631
Garnet	0.15673	0.15110	0.26423	0.13307	0.09221
Pyrite	0.00592	0.01043	0.00645	0.00670	0.00727
Sphalerite	0.00000	0.00000	0.00037	0.00000	0.00001
Chalcopyrite	0.00218	0.00075	0.00078	0.00125	0.00100
Fe-oxide	0.01198	0.00219	0.00220	0.00170	0.00161
Chromite	0.00116	0.00083	0.00139	0.00015	0.00094
Titanite	0.00020	0.00136	0.00509	0.00150	0.00015
Epidote	0.00000	0.00000	0.00000	0.00000	0.00000
Zoisite	0.00000	0.00000	0.00000	0.00000	0.00000
Olivine	0.00000	0.00000	0.00000	0.00000	0.00022
Xenotime-(Y)	0.00025	0.00009	0.00006	0.00017	0.00007
Ilmenite	0.05518	0.01775	0.01003	0.01545	0.03099
Ilmenorutile	0.05459	0.05226	0.05641	0.04735	0.05082
Rutile	0.07933	0.08295	0.08753	0.07339	0.08625
Rutile-Ilm mix	0.18453	0.18009	0.20992	0.14518	0.21641
Monazite-(Ce)	0.00413	0.00737	0.00460	0.00811	0.00717
Zircon	0.04665	0.03824	0.04429	0.03899	0.04206
Thorite	0.00001	0.00000	0.00082	0.00040	0.00143
Calc-qtz-mix	0.00000	0.00000	0.00000	0.00000	0.06474
Organic	0.55288	0.40742	0.88756	0.41405	0.43438
Clay	0.00000	0.00000	0.00000	0.00000	0.00000
Pores	1.88666	0.65491	0.18674	0.32933	0.30516
Unknown	0.00506	0.00286	0.02102	0.00000	0.00000
Low_Counts	0.00000	0.00000	0.00012	0.00000	0.00000
No_XRay	0.00010	0.00003	0.00001	0.00003	0.00001
Total	100.00000	100.00000	100.00000	100.00000	100.00000

SEM-MLA data of samples in Area% of thin-section (ungrouped)

Mineral	BOI16_B9	BOI16_B10	BOI16_B11	BOI16-B12	BOI16-B13
Quartz	49.92677	60.22719	21.79970	35.24191	51.45270
Plagioclase	0.02820	0.01011	0.88746	0.00525	0.00665
Albite	16.08670	17.20101	24.73953	25.27485	13.86176
K-spar	9.54355	7.56981	10.63385	9.41756	8.11511
Calcite	0.63449	0.14361	21.77532	0.00739	0.02906
Siderite	0.00000	0.00010	0.00001	0.00000	0.00000
Ankerite	0.06637	0.01169	1.85649	0.00276	0.00446
Dolomite	0.00000	0.00000	0.00000	0.00000	0.00022
Apatite	0.07905	0.05445	0.03990	0.10381	0.04372
Phosph. Shale	0.08983	0.03432	0.88873	0.03899	0.03213
Barite	0.00818	0.00032	0.00053	0.00663	0.00263
Muscovite	0.27571	0.18491	0.37674	0.69524	0.33380
Biotite	0.77475	0.25408	0.40120	0.74596	0.95284
Chlorit-Fe	6.42471	5.99736	6.71339	7.73020	6.81542
Kaolinite	0.00393	0.00612	0.00322	0.00433	0.00317
Illite	13.73635	6.74020	7.48115	18.72015	16.20014
Glauconite	0.06477	0.02628	0.02571	0.00777	0.01362
Clinochlore	0.01418	0.00834	0.01825	0.00992	0.00729
Garnet	0.12214	0.26807	0.01386	0.01236	0.10491
Pyrite	0.01156	0.01454	0.00581	0.02061	0.01029
Sphalerite	0.00000	0.00000	0.00017	0.00009	0.00000
Chalcopyrite	0.00264	0.00111	0.00050	0.00440	0.00146
Fe-oxide	0.00446	0.00285	0.00065	0.00024	0.00070
Chromite	0.00149	0.00211	0.00006	0.00135	0.00024
Titanite	0.00126	0.00310	0.00947	0.00024	0.00023
Epidote	0.00000	0.00000	0.00000	0.00000	0.00000
Zoisite	0.00000	0.00000	0.00000	0.00000	0.00000
Olivine	0.00000	0.00000	0.00000	0.00000	0.00012
Xenotime-(Y)	0.00018	0.00045	0.00003	0.00007	0.00168
Ilmenite	0.01328	0.05060	0.00141	0.00545	0.00267
Ilmenorutile	0.06604	0.07461	0.03062	0.10807	0.06255
Rutile	0.09042	0.17581	0.03656	0.17390	0.07895
Rutile-Ilm mix	0.18418	0.35782	0.07085	0.24552	0.22173
Monazite-(Ce)	0.00253	0.00897	0.00121	0.00684	0.00388
Zircon	0.02962	0.08958	0.00920	0.06994	0.04520
Thorite	0.00000	0.02199	0.00000	0.00000	0.00012
Calc-qtz-mix	0.00000	0.00000	0.00000	0.00112	0.01328
Organic	0.76481	0.28248	2.04618	0.87847	0.65309
Clay	0.00000	0.00000	0.00000	0.00000	0.00000
Pores	0.94138	0.16938	0.12812	0.45671	0.92417
Unknown	0.00645	0.00664	0.00408	0.00182	0.00000
Low_Counts	0.00000	0.00000	0.00000	0.00000	0.00000
No_XRay	0.00003	0.00001	0.00001	0.00011	0.00004
Total	100.00000	100.00000	100.00000	100.00000	100.00000

SEM-MLA data of samples in Area% of thin-section (ungrouped)

Mineral	BOI16-B14	BOI16-B15	BOI16-B16	PAP16-CC3	PAP16-MF10
Quartz	51.13842	34.39027	34.56330	11.27	27.96
Plagioclase	0.01816	0.00172	0.29182	0.19	0.15
Albite	21.10785	13.14209	23.61547	0.82	16.62
K-spar	5.24336	0.11716	9.33681	1.06	4.79
Calcite	0.37012	0.00072	4.30934	28.35	5.84
Siderite	0.00706	0.00018	0.00012	0.00	0.00
Ankerite	0.05144	0.00024	0.60056	6.67	2.01
Dolomite	0.00000	0.00000	0.00000	33.43	2.16
Apatite	0.03589	0.04120	0.05389	0.03	0.12
Phosph. Shale	0.02823	0.04602	0.68827	0.10	0.61
Barite	0.00383	0.00209	0.00201	0.00	0.03
Muscovite	0.26375	2.32932	0.35388	0.00	0.08
Biotite	0.43634	1.82501	1.42675	0.00	0.24
Chlorit-Fe	7.47849	7.56754	7.18869	0.18	28.63
Kaolinite	0.00244	0.00284	0.00397	0.00	0.00
Illite	12.20199	36.78120	14.66885	0.04	3.25
Glauconite	0.03287	0.00000	0.00625	0.00	1.98
Clinochlore	0.00963	0.01175	0.01603	0.00	0.08
Garnet	0.06858	0.02241	0.02765	0.00	0.00
Pyrite	0.01372	0.09566	0.00839	0.08	0.06
Sphalerite	0.00000	0.00000	0.00000	0.00	0.00
Chalcopyrite	0.00068	0.00273	0.00287	0.00	0.00
Fe-oxide	0.00366	0.00177	0.04651	0.00	0.00
Chromite	0.00042	0.00081	0.00068	0.00	0.01
Titanite	0.00064	0.00012	0.00360	0.00	0.01
Epidote	0.00000	0.00000	0.00000	0.00	0.00
Zoisite	0.00000	0.00000	0.00000	0.00	0.00
Olivine	0.00036	0.00030	0.00018	0.00	0.00
Xenotime-(Y)	0.00000	0.00008	0.00043	0.00	0.00
Ilmenite	0.03807	0.00046	0.02938	0.00	0.00
Ilmenorutile	0.03490	0.06813	0.06345	0.00	0.04
Rutile	0.07287	0.06436	0.08871	0.00	0.05
Rutile-Ilm mix	0.07538	0.06972	0.10482	0.00	0.04
Monazite-(Ce)	0.00409	0.00282	0.00247	0.00	0.00
Zircon	0.02295	0.01975	0.02645	0.00	0.01
Thorite	0.00000	0.00000	0.00000	0.00	0.00
Calc-qtz-mix	0.04597	0.00359	0.46700	16.80	0.79
Organic	0.60811	1.25048	1.66393	0.95	3.82
Clay	0.00000	0.00000	0.00000	0.00	0.00
Pores	0.57648	2.13730	0.33597	0.01	0.63
Unknown	0.00325	0.00000	0.00151	0.01	0.00
Low_Counts	0.00000	0.00000	0.00000	0.00	0.00
No_XRay	0.00002	0.00015	0.00003	0.00	0.00
Total	100.00000	100.00000	100.00000	100.00	100.00

SEM-MLA data of samples in Area% of thin-section (ungrouped)

Mineral	PAP16-MF12	PAP16-MF14	PAP16-MF15	PAP16-MF18b
Quartz	3.34	63.07	45.86	32.45
Plagioclase	0.06	0.05	0.08	0.14
Albite	0.59	4.67	13.05	17.79
K-spar	1.04	4.15	7.22	4.71
Calcite	45.32	6.22	4.54	4.95
Siderite	0.00	0.00	0.00	0.00
Ankerite	6.67	0.93	0.98	1.74
Dolomite	36.78	0.18	0.47	1.33
Apatite	0.02	0.07	0.12	0.13
Phosph. Shale	0.61	0.20	0.31	0.45
Barite	0.00	0.00	0.00	0.00
Muscovite	0.00	0.02	0.09	0.08
Biotite	0.00	0.03	0.23	0.21
Chlorit-Fe	0.84	6.26	18.68	26.33
Kaolinite	0.00	0.00	0.00	0.00
Illite	0.14	0.40	2.55	3.14
Glauconite	0.05	0.88	0.85	1.30
Clinochlore	0.00	0.23	0.24	0.08
Garnet	0.00	0.00	0.00	0.00
Pyrite	0.03	0.87	0.31	0.09
Sphalerite	0.00	0.00	0.00	0.00
Chalcopyrite	0.00	0.00	0.00	0.00
Fe-oxide	0.00	0.00	0.00	0.00
Chromite	0.00	0.03	0.04	0.02
Titanite	0.00	0.00	0.00	0.00
Epidote	0.00	0.00	0.00	0.00
Zoisite	0.00	0.00	0.00	0.00
Olivine	0.00	0.00	0.00	0.00
Xenotime-(Y)	0.00	0.00	0.00	0.00
Ilmenite	0.00	0.00	0.00	0.00
Ilmenorutile	0.00	0.02	0.05	0.04
Rutile	0.00	0.02	0.09	0.06
Rutile-Ilm mix	0.01	0.01	0.05	0.04
Monazite-(Ce)	0.00	0.00	0.00	0.00
Zircon	0.00	0.01	0.02	0.02
Thorite	0.00	0.00	0.00	0.00
Calc-qtz-mix	2.94	0.34	0.39	0.68
Organic	1.41	1.53	2.36	3.68
Clay	0.00	0.00	0.00	0.00
Pores	0.11	9.80	1.39	0.54
Unknown	0.00	0.00	0.00	0.00
Low_Counts	0.00	0.00	0.00	0.00
No_XRay	0.00	0.00	0.00	0.00
Total	100.00	100.00	100.00	100.00

SEM-MLA data of samples in Area% of thin-section (grouped)

Mineral	BOI16_B1	BOI16_B2	BOI16_B3a	BOI16_B3b	BOI16_B4
Rigid	64.2394	59.1019	68.5962	64.5682	64.1094
Ductile	20.9021	15.2337	17.1675	17.0209	19.8010
Matrix	14.3869	23.0728	14.1745	18.0963	15.8973
Pores	0.4686	2.5916	0.0600	0.3110	0.1922
Low_Counts	0.0000	0.0000	0.0000	0.0000	0.0000
Unknown	0.0030	0.0000	0.0017	0.0036	0.0000
No_XRay	0.0000	0.0001	0.0000	0.0000	0.0000
Total	100.0000	100.0000	100.0000	100.0000	100.0000

Mineral	BOI16_B5	BOI16_B6	BOI16_B7	BOI16_B8a	BOI16-B8b
Rigid	63.2506	68.6711	67.7694	67.9067	69.4061
Ductile	15.9766	14.8880	12.6372	16.3672	15.1846
Matrix	18.8810	15.7831	19.3855	15.3968	15.1041
Pores	1.8867	0.6549	0.1867	0.3293	0.3052
Low_Counts	0.0000	0.0000	0.0001	0.0000	0.0000
Unknown	0.0051	0.0029	0.0210	0.0000	0.0000
No_XRay	0.0001	0.0000	0.0000	0.0000	0.0000
Total	100.0000	100.0000	100.0000	100.0000	100.0000

Mineral	BOI16_B9	BOI16_B10	BOI16_B11	BOI16-B12	BOI16-B13
Rigid	60.0055	68.8454	32.6138	45.3106	60.1019
Ductile	17.4018	17.7887	27.3600	26.8764	15.2478
Matrix	21.6448	13.1899	39.8940	27.3543	23.7261
Pores	0.9414	0.1694	0.1281	0.4567	0.9242
Low_Counts	0.0000	0.0000	0.0000	0.0000	0.0000
Unknown	0.0065	0.0066	0.0041	0.0018	0.0000
No_XRay	0.0000	0.0000	0.0000	0.0001	0.0000
Total	100.0000	100.0000	100.0000	100.0000	100.0000

Mineral	BOI16-B15	BOI16-B16	PAP16-CC3	PAP16-MF10	PAP16-MF12
Rigid	34.8558	44.3044	12.4	33.0	4.4
Ductile	17.3882	26.4396	1.1	19.8	1.3
Matrix	45.6185	28.9185	86.4	46.6	94.1
Pores	2.1373	0.3360	0.0	0.6	0.1
Low_Counts	0.0000	0.0000	0.0	0.0	0.0
Unknown	0.0000	0.0015	0.0	0.0	0.0
No_XRay	0.0001	0.0000	0.0	0.0	0.0
Total	100.0000	100.0000	100.0	100.0	100.0

Mineral	PAP16-MF14	PAP16-MF15	PAP16-MF18b
Rigid	68.2	53.7	37.4
Ductile	5.9	14.7	20.1
Matrix	16.1	30.2	41.9
Pores	9.8	1.4	0.5
Low_Counts	0.0	0.0	0.0
Unknown	0.0	0.0	0.0
No_XRay	0.0	0.0	0.0
Total	100.0	100.0	100.0